

A Dynamical System Analysis of cosmic evolution with coupled phantom dark energy with dark matter

Soumya Chakraborty,^{*} Sudip Mishra,[†] and Subenoy Chakraborty[‡]
Department of Mathematics, Jadavpur University, Kolkata- 700032, WB, India.

The present work is an example of the application of the dynamical system analysis in the context of cosmology. Here cosmic evolution is considered in the background of homogeneous and isotropic flat Friedmann-Lemaître-Robertson-Walker space-time with interacting dark energy and varying mass dark matter as the matter content. The DE is chosen as phantom scalar field with self-interacting potential while the DM is in the form of dust. The potential of the scalar field and the mass function of dark matter are chosen as exponential or power-law form or in their product form. Using suitable dimensionless variables the Einstein field equations and the conservation equations constitute an autonomous system. The stability of the non-hyperbolic critical points are analyzed by using center manifold theory. Finally, cosmological phase transitions have been detected through bifurcation analysis which has been done by Poincaré index theory.

arXiv:2011.09842v1 [gr-qc] 18 Nov 2020

^{*} soumyachakraborty150@gmail.com

[†] corresponding author: sudipcmiitmath@gmail.com

[‡] schakraborty.math@gmail.com

I. INTRODUCTION

The unexpected accelerated expansion of the universe as predicted by recent series of observations is speculated by cosmologist as a smooth transition from decelerated era in recent past [1–5]. The cosmologists are divided in opinion about the cause of this transition. One group has the opinion of modification of the gravity theory while others are in favour introducing exotic matter component. Due to two severe drawbacks [6] of the cosmological constant as a DE candidate dynamical DE models namely quintessence field (canonical scalar field), phantom field [7–11] (ghost scalar field) or a unified model named quintom [12–14] are popular in the literature.

However, a new cosmological problem arises due to the dynamical nature of the DE although vacuum energy and DM scale independently during cosmic evolution but why their energy densities are nearly equal today. To resolve this coincidence problem cosmologists introduce interaction between the DE and DM. As the choice of this interaction is purely phenomenological so various models appear to match the observational prediction. Although these models may resolve the above coincidence problem but a non-trivial, almost tuned sequence of cosmological eras [15] appear as a result. Further, the interacting phantom DE models [16–22] deal with some special coupling forms, alleviating the coincidence problem.

Alternatively cosmologists put forward with a special type of interaction between DE and DM where the DM particles has variable mass, depending on the scalar field representing the DE [23]. Such type of interacting model is physically more sound as scalar field dependent varying mass model appears in string theory or scalar-tensor theory [24]. This type of interacting model in cosmology considers mass variation as linear [23, 25, 26], power law [27] or exponential [28–34] on the scalar field. Among these the exponential dependence is most suitable as it not only solves the coincidence problem but also gives stable scaling behaviour.

In the present work, varying mass interacting DE/DM model is considered in the background of homogeneous and isotropic space-time model. Due to highly coupled nonlinear nature of the Einstein field equations it is not possible to have any analytic solution. So by using suitable dimensionless variables the field equations are converted to an autonomous system. The phase space analysis of non-hyperbolic equilibrium points has been done by center manifold theory (CMT) for various choices of the mass functions and the scalar field potentials. The paper is organized as follows: Section II deals with basic equations for the varying mass interacting dark energy and dark matter cosmological model. Autonomous system is formed and critical points are determined in Section III. Also stability analysis of all critical points for various choices of the involving parameters are shown in this section. Possible bifurcation scenarios [35–37] by Poincaré index theory and global cosmological evolution have been examined in Section IV. Finally, brief discussion and important concluding remarks of the present work is proposed in Section V.

II. VARYING MASS INTERACTING DARK ENERGY AND DARK MATTER COSMOLOGICAL MODEL : BASIC EQUATIONS

Throughout this paper, we assume a homogeneous and isotropic universe with the flat Friedmann-Lemaître-Robertson-Walker (FLRW) metric as follows:

$$ds^2 = -dt^2 + a^2(t) d\Sigma^2, \quad (1)$$

where ‘ t ’ is the comoving time; $a(t)$ is the scale factor; $d\Sigma^2$ is the 3D flat space line element. The Friedmann equations in the background of flat FLRW metric can be expressed as

$$3H^2 = \kappa^2(\rho_\phi + \rho_{DM}), \quad (2)$$

$$2\dot{H} = -\kappa^2(\rho_\phi + p_\phi + \rho_{DM}), \quad (3)$$

where ‘ $\dot{}$ ’ denotes the derivative with respect to t ; $\kappa (= \sqrt{8\pi G})$ is the gravitational coupling; $\{\rho_\phi, p_\phi\}$ are the energy density and thermodynamic pressure of the phantom scalar field ϕ (considered as DE) having expressions

$$\begin{aligned} \rho_\phi &= -\frac{1}{2}\dot{\phi}^2 + V(\phi), \\ p_\phi &= -\frac{1}{2}\dot{\phi}^2 - V(\phi), \end{aligned} \quad (4)$$

and ρ_{DM} is the energy density for the dark matter in the form of dust having expression

$$\rho_{DM} = M_{DM}(\phi)n_{DM}, \quad (5)$$

where n_{DM} , the number density [38] for DM satisfies the number conservation equation

$$\dot{n}_{DM} + 3Hn_{DM} = 0. \quad (6)$$

Now differentiating (5) and using (6) one has the DM conservation equation as

$$\dot{\rho}_{DM} + 3H\rho_{DM} = \frac{d}{d\phi} \{ \ln M_{DM}(\phi) \} \dot{\phi} \rho_{DM}, \quad (7)$$

which shows that mass varying DM (in the form of dust) can be interpreted as a barotropic fluid with variable equation of state : $\omega_{DM} = \frac{d}{d\phi} \{ \ln M_{DM}(\phi) \} \dot{\phi}$. Now due to Bianchi identity, using the Einstein field equations (2) and (3) the conservation equation for DE takes the form

$$\dot{\rho}_\phi + 3H(\rho_\phi + p_\phi) = -\frac{d}{d\phi} \{ \ln M_{DM}(\phi) \} \dot{\phi} \rho_{DM}. \quad (8)$$

or using (4) one has

$$\ddot{\phi} + 3H\dot{\phi} - \frac{\partial V}{\partial \phi} = \frac{d}{d\phi} \{ \ln M_{DM}(\phi) \} \rho_{DM}. \quad (9)$$

The combination of the conservation equations (7) and (8) for DM (dust) and phantom DE (scalar) shows that the interaction between these two matter components depends purely on the mass variation, i.e., $Q = \frac{d}{d\phi} \{ \ln M_{DM}(\phi) \} \rho_{DM}$. So, if M_{DM} is an increasing function of ϕ , i.e., $Q > 0$ then energy is exchanged from DE to DM while in the opposite way if M_{DM} is a decreasing function of ϕ . Further, combining equations (7) and (8) the total matter $\rho_{tot} = \rho_{DM} + \rho_{DE}$ satisfies

$$\dot{\rho}_{tot} + 3H(\rho_{tot} + p_{tot}) = 0 \quad (10)$$

with

$$\omega_{tot} = \frac{p_\phi}{\rho_\phi + \rho_{DM}} = \omega_\phi \Omega_\phi. \quad (11)$$

Here $\omega_\phi = \frac{p_\phi}{\rho_\phi}$ is the equation of state parameter for phantom field and $\Omega_\phi = \frac{\rho_\phi}{\frac{3H^2}{\kappa^2}}$ is the density parameter for DE.

III. FORMATION OF AUTONOMOUS SYSTEM : CRITICAL POINT AND STABILITY ANALYSIS

In the present work the dimensionless variables can be taken as [38]

$$x := \frac{\kappa \dot{\phi}}{\sqrt{6}H}, \quad (12)$$

$$y := \frac{\kappa \sqrt{V(\phi)}}{\sqrt{3}H}, \quad (13)$$

$$z := \frac{\sqrt{6}}{\kappa \phi} \quad (14)$$

together with $N = \ln a$ and the expression of the cosmological parameters can be written as

$$\Omega_\phi \equiv \frac{\kappa^2 \rho_\phi}{3H^2} = -x^2 + y^2, \quad (15)$$

$$\omega_\phi = \frac{-x^2 - y^2}{-x^2 + y^2} \quad (16)$$

and

$$\omega_{tot} = -x^2 - y^2. \quad (17)$$

For the scalar field potential we consider two well studied cases in the literature, namely the power-law

$$V(\phi) = V_0\phi^{-\lambda} \quad (18)$$

and the exponential dependence as

$$V(\phi) = V_1e^{-\kappa\lambda\phi}. \quad (19)$$

For the dark matter particle mass we also consider power-law

$$M_{DM}(\phi) = M_0\phi^{-\mu} \quad (20)$$

and the exponential dependence as

$$M_{DM}(\phi) = M_1e^{-\kappa\mu\phi}, \quad (21)$$

where $V_0, V_1, M_0, M_1 (> 0)$ and λ, μ are constant parameters. Here we study the dynamical analysis of this cosmological system for five possible models. In Model 1 (III A) we consider $V(\phi) = V_0\phi^{-\lambda}, M_{DM}(\phi) = M_0\phi^{-\mu}$, in Model 2 (III B) we consider $V(\phi) = V_0\phi^{-\lambda}, M_{DM}(\phi) = M_1e^{-\kappa\mu\phi}$, in Model 3 (III C) we consider $V(\phi) = V_1e^{-\kappa\lambda\phi}, M_{DM}(\phi) = M_0\phi^{-\mu}$, in Model 4 (III D) we consider $V(\phi) = V_1e^{-\kappa\lambda\phi}, M_{DM}(\phi) = M_1e^{-\kappa\mu\phi}$ and lastly in Model 5 (III E) we consider $V(\phi) = V_2\phi^{-\lambda}e^{-\kappa\lambda\phi}, M_{DM}(\phi) = M_2\phi^{-\mu}e^{-\kappa\mu\phi}$, where $V_2 = V_0V_1$ and $M_2 = M_0M_1$.

A. Model 1: Power-law potential and power-law-dependent dark-matter particle mass

In this consideration evolution equations in Section II can be converted to an autonomous system as follows

$$x' = -3x + \frac{3}{2}x(1 - x^2 - y^2) - \frac{\lambda y^2 z}{2} - \frac{\mu}{2}z(1 + x^2 - y^2), \quad (22)$$

$$y' = \frac{3}{2}y(1 - x^2 - y^2) - \frac{\lambda xyz}{2}, \quad (23)$$

$$z' = -xz^2, \quad (24)$$

where ‘dash’ over a variable denotes differentiation with respect to $N = \ln a$.

To obtain the stability analysis of the critical points corresponding to the autonomous system (22 – 24), we consider four possible choices of μ and λ as (i) $\mu \neq 0$ and $\lambda \neq 0$, (ii) $\mu \neq 0$ and $\lambda = 0$, (iii) $\mu = 0$ and $\lambda \neq 0$, (iv) $\mu = 0$ and $\lambda = 0$.

Case-(i) $\mu \neq 0$ and $\lambda \neq 0$

In this case we have three real and physically meaningful critical points $A_1(0, 0, 0)$, $A_2(0, 1, 0)$ and $A_3(0, -1, 0)$. First we determine the Jacobian matrix at these critical points corresponding to the autonomous system (22–24). Then we shall find the eigenvalues and corresponding eigenvectors of the Jacobian matrix. After that we shall obtain the nature of the vector field near the origin for every critical points. If the critical point is hyperbolic in nature we use Hartman-Grobman theorem and if the critical point is non-hyperbolic in nature we use Center Manifold Theory [39]. At every critical points the eigenvalues of the Jacobian matrix corresponding to the autonomous system (22 – 24), value of cosmological parameters and the nature of the critical points are shown in Table I.

1. Critical Point A_1

The Jacobian matrix at the critical point A_1 can be put as

$$J(A_1) = \begin{bmatrix} -\frac{3}{2} & 0 & -\frac{\mu}{2} \\ 0 & \frac{3}{2} & 0 \\ 0 & 0 & 0 \end{bmatrix}. \quad (25)$$

The eigenvalues of $J(A_1)$ are $-\frac{3}{2}, \frac{3}{2}$ and 0. $[1, 0, 0]^T$, $[0, 1, 0]^T$ and $[-\frac{\mu}{3}, 0, 1]^T$ are the eigenvectors corresponding to the eigenvalues $-\frac{3}{2}, \frac{3}{2}$ and 0 respectively. Since the critical point A_1 is non-hyperbolic in nature, so we use

TABLE I: Table shows the eigenvalues, cosmological parameters and nature of the critical points corresponding to each critical points ($A_1 - A_3$).

<i>Critical Points</i>	λ_1	λ_2	λ_3	Ω_ϕ	ω_ϕ	ω_{tot}	q	<i>Nature of critical points</i>
$A_1(0, 0, 0)$	$-\frac{3}{2}$	$\frac{3}{2}$	0	0	Undetermined	0	$\frac{1}{2}$	Non-hyperbolic
$A_2(0, 1, 0)$	-3	-3	0	1	-1	-1	-1	Non-hyperbolic
$A_3(0, -1, 0)$	-3	-3	0	1	-1	-1	-1	Non-hyperbolic

Center Manifold Theory for analyzing the stability of this critical point. From the entries of the Jacobian matrix we can see that there is a linear term of z corresponding to the eqn.(22) of the autonomous system (22 – 24). But the eigen value 0 of the Jacobian matrix (25) is corresponding to (24). So we have to introduce another coordinate system (X, Y, Z) in terms of (x, y, z). By using the eigenvectors of the Jacobian matrix (25), we introduce the following coordinate system

$$\begin{bmatrix} X \\ Y \\ Z \end{bmatrix} = \begin{bmatrix} 1 & 0 & \frac{\mu}{3} \\ 0 & 1 & 0 \\ 0 & 0 & 1 \end{bmatrix} \begin{bmatrix} x \\ y \\ z \end{bmatrix} \quad (26)$$

and in these new coordinate system the equations (22 – 24) are transformed into

$$\begin{bmatrix} X' \\ Y' \\ Z' \end{bmatrix} = \begin{bmatrix} -\frac{3}{2} & 0 & 0 \\ 0 & \frac{3}{2} & 0 \\ 0 & 0 & 0 \end{bmatrix} \begin{bmatrix} X \\ Y \\ Z \end{bmatrix} + \begin{bmatrix} \text{non} \\ \text{linear} \\ \text{terms} \end{bmatrix}. \quad (27)$$

By Center Manifold Theory there exists a continuously differentiable function $h: \mathbb{R} \rightarrow \mathbb{R}^2$ such that

$$h(Z) = \begin{bmatrix} X \\ Y \end{bmatrix} = \begin{bmatrix} a_1 Z^2 + a_2 Z^3 + a_3 Z^4 + \mathcal{O}(Z^5) \\ b_1 Z^2 + b_2 Z^3 + a_3 Z^4 + \mathcal{O}(Z^5) \end{bmatrix}. \quad (28)$$

Differentiating both side with respect to N , we get

$$X' = (2a_1 Z + 3a_2 Z^2 + 4a_3 Z^3) Z', \quad (29)$$

$$Y' = (2b_1 Z + 3b_2 Z^2 + 4b_3 Z^3) Z', \quad (30)$$

where $a_i, b_i \in \mathbb{R}$. We only concern about the non-zero coefficients of the lowest power terms in CMT as we analyze arbitrary small neighbourhood of the origin. Comparing coefficients corresponding to power of Z we get, $a_1=0, a_2 = \frac{2\mu^2}{27}, a_3 = 0$ and $b_i=0$ for all i . So, the center manifold is given by

$$X = \frac{2\mu^2}{27} Z^3, \quad (31)$$

$$Y = 0 \quad (32)$$

and the flow on the Center manifold is determined by

$$Z' = \frac{\mu}{3} Z^3 + \mathcal{O}(Z^5). \quad (33)$$

The flow on the center manifold depends on the sign of μ . If $\mu > 0$ then $Z' > 0$ for $Z > 0$ and $Z' < 0$ for $Z < 0$. Hence, we conclude that for $\mu > 0$ the origin is a saddle node and unstable in nature (FIG.1(a)). Again if $\mu < 0$ then $Z' < 0$ for $Z > 0$ and $Z' > 0$ for $Z < 0$. So, we conclude that for $\mu < 0$ the origin is a stable node, i.e., stable in nature (FIG.1(b)).

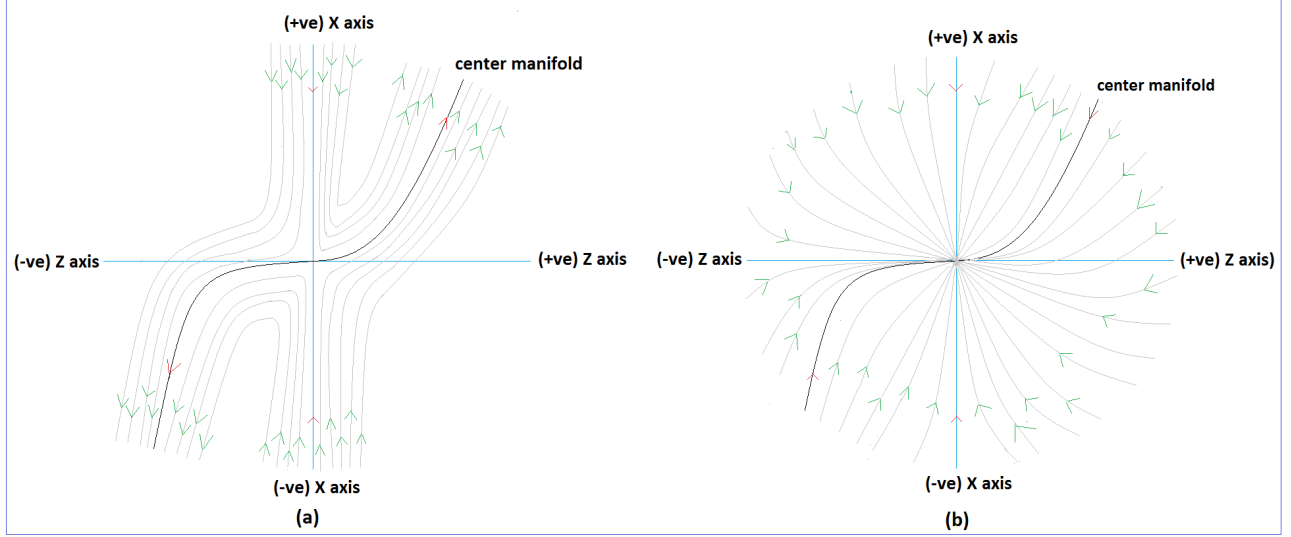


FIG. 1: Vector field near the origin for the critical point A_1 in XZ -plane. L.H.S. figure is for $\mu > 0$ and R.H.S. figure is for $\mu < 0$.

2. Critical Point A_2

The Jacobian matrix at A_2 can be put as

$$J(A_2) = \begin{bmatrix} -3 & 0 & -\frac{\lambda}{2} \\ 0 & -3 & 0 \\ 0 & 0 & 0 \end{bmatrix}. \quad (34)$$

The eigenvalues of the above matrix are -3 , -3 and 0 . $[1, 0, 0]^T$ and $[0, 1, 0]^T$ are the eigenvectors corresponding to the eigenvalue -3 and $[-\frac{\lambda}{6}, 0, 1]^T$ be the eigenvector corresponding to the eigenvalue 0 . Since the critical point A_2 is non-hyperbolic in nature, so we use Center Manifold Theory for analyzing the stability of this critical point. We first transform the coordinates into a new system $x = X$, $y = Y + 1$, $z = Z$, such that the critical point A_2 moves to the origin. By using the eigenvectors of the Jacobian matrix $J(A_2)$, we introduce another set of new coordinates (u, v, w) in terms of (X, Y, Z) as

$$\begin{bmatrix} u \\ v \\ w \end{bmatrix} = \begin{bmatrix} 1 & 0 & \frac{\lambda}{6} \\ 0 & 1 & 0 \\ 0 & 0 & 1 \end{bmatrix} \begin{bmatrix} X \\ Y \\ Z \end{bmatrix} \quad (35)$$

and in these new coordinates the equations (22 – 24) are transformed into

$$\begin{bmatrix} u' \\ v' \\ w' \end{bmatrix} = \begin{bmatrix} -3 & 0 & 0 \\ 0 & -3 & 0 \\ 0 & 0 & 0 \end{bmatrix} \begin{bmatrix} u \\ v \\ w \end{bmatrix} + \begin{bmatrix} \text{non} \\ \text{linear} \\ \text{terms} \end{bmatrix}. \quad (36)$$

By center manifold theory there exists a continuously differentiable function $h: \mathbb{R} \rightarrow \mathbb{R}^2$ such that

$$h(w) = \begin{bmatrix} u \\ v \end{bmatrix} = \begin{bmatrix} a_1 w^2 + a_2 w^3 + \mathcal{O}(w^4) \\ b_1 w^2 + b_2 w^3 + \mathcal{O}(w^4) \end{bmatrix}. \quad (37)$$

Differentiating both side with respect to N , we get

$$u' = (2a_1 w + 3a_2 w^2)w' + \mathcal{O}(w^3) \quad (38)$$

$$v' = (2b_1 w + 3b_2 w^2)w' + \mathcal{O}(w^3) \quad (39)$$

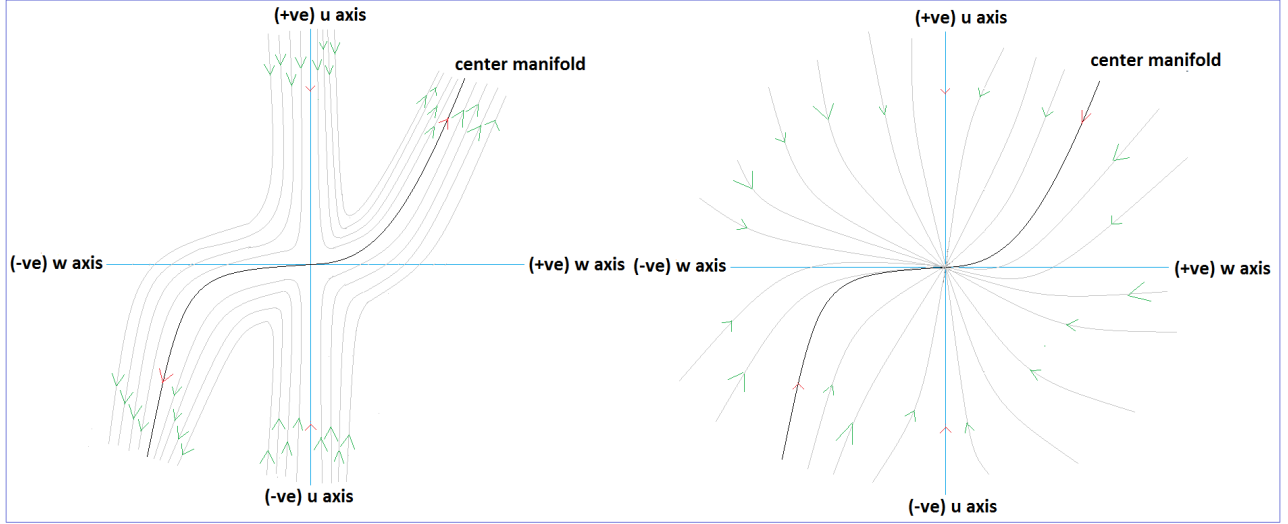


FIG. 2: Vector field near the origin for the critical point A_2 in (uw) -plane. L.H.S. figure is for $\lambda > 0$ and R.H.S. figure is for $\lambda < 0$.

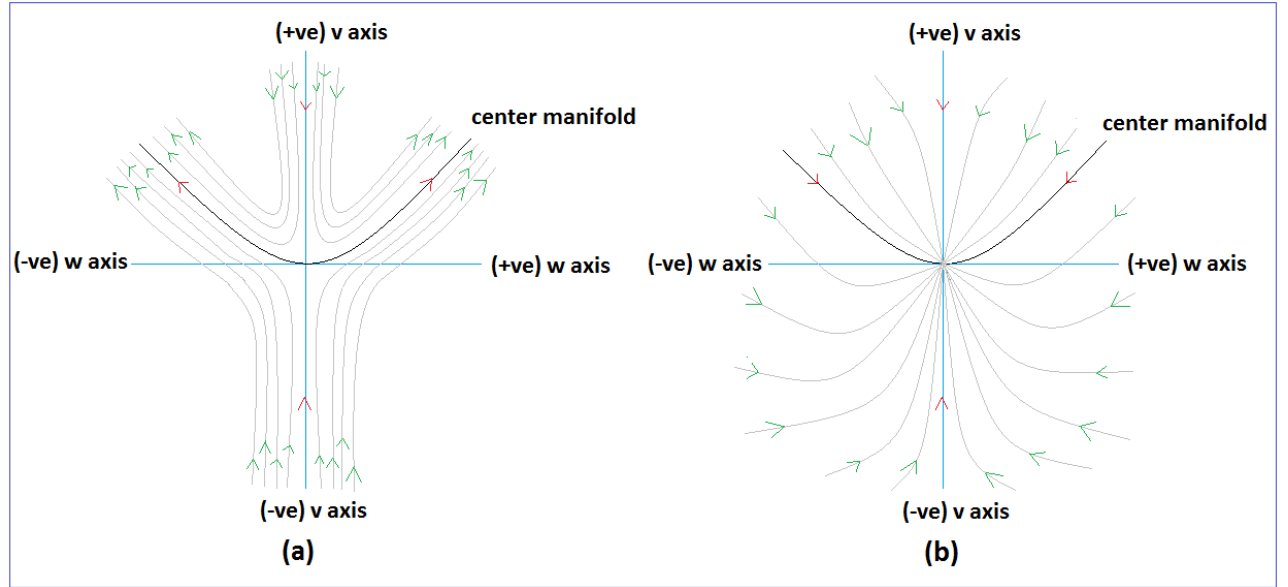


FIG. 3: Vector field near the origin for the critical point A_2 in (vw) -plane. L.H.S. figure is for $\lambda > 0$ and R.H.S. figure is for $\lambda < 0$.

where $a_i, b_i \in \mathbb{R}$. We only concern about the non-zero coefficients of the lowest power terms in CMT as we analyze arbitrary small neighbourhood of the origin. Comparing coefficients corresponding to power of w both sides of (38) and (39), we get $a_1=0$, $a_2 = \frac{\lambda^2}{108}$ and $b_1 = \frac{\lambda^2}{72}$, $b_2 = 0$. So, the center manifold can be written as

$$u = \frac{\lambda^2}{108} w^3, \quad (40)$$

$$v = \frac{\lambda^2}{72} w^2 \quad (41)$$

and the flow on the center manifold is determined by

$$w' = \frac{\lambda}{6} w^3 + \mathcal{O}(w^4). \quad (42)$$

Here we see the center manifold and the flow on the center manifold is completely same as the center manifold and the flow which was determined in [40] and the stability of the vector field near the origin depends on the sign of λ . If $\lambda < 0$ then $w' < 0$ for $w > 0$ and $w' > 0$ for $w < 0$. So, for $\lambda < 0$ the origin is a stable node,

i.e., stable in nature. Again if $\lambda > 0$ then $w' > 0$ for $w > 0$ and $w' < 0$ for $w < 0$. So, for $\lambda > 0$ the origin is a saddle node, i.e., unstable in nature. The vector field near the origin are shown as in FIG.2 and FIG.3 separately for (wu) -plane and (wv) -plane respectively. As the new coordinate system (u, v, w) is topologically equivalent to the old one, hence the origin in the new coordinate system, i.e., the critical point A_2 in the old coordinate system (x, y, z) is a stable node for $\lambda < 0$ and a saddle node for $\lambda > 0$.

3. Critical Point A_3

The Jacobian matrix at the critical point A_3 is same as (34). So, the eigenvalues and corresponding eigenvectors are also same as above. Now we transform the coordinates into a new system $x = X, y = Y - 1, z = Z$, such that the critical point is at the origin. Then by using the matrix transformation (35) and after putting similar arguments as above, the expressions of the center manifold can be written as

$$u = -\frac{\lambda^2}{108}w^3, \quad (43)$$

$$v = -\frac{\lambda^2}{72}w^2 \quad (44)$$

and the flow on the center manifold is determined by

$$w' = \frac{\lambda}{6}w^3 + \mathcal{O}(w^4). \quad (45)$$

Here also the stability of the vector field near the origin depends on the sign of λ . Again as the expression of the flow on the center manifold is same as (42). So we can conclude as above that for $\lambda < 0$ the origin is a stable node, i.e., stable in nature and for $\lambda > 0$ the origin is unstable due to its saddle nature. The vector fields near the origin on uw -plane and vw -plane are shown as in FIG.4 and FIG.5 respectively. Hence, the critical point A_3 is a stable node for $\lambda < 0$ and a saddle node for $\lambda > 0$.

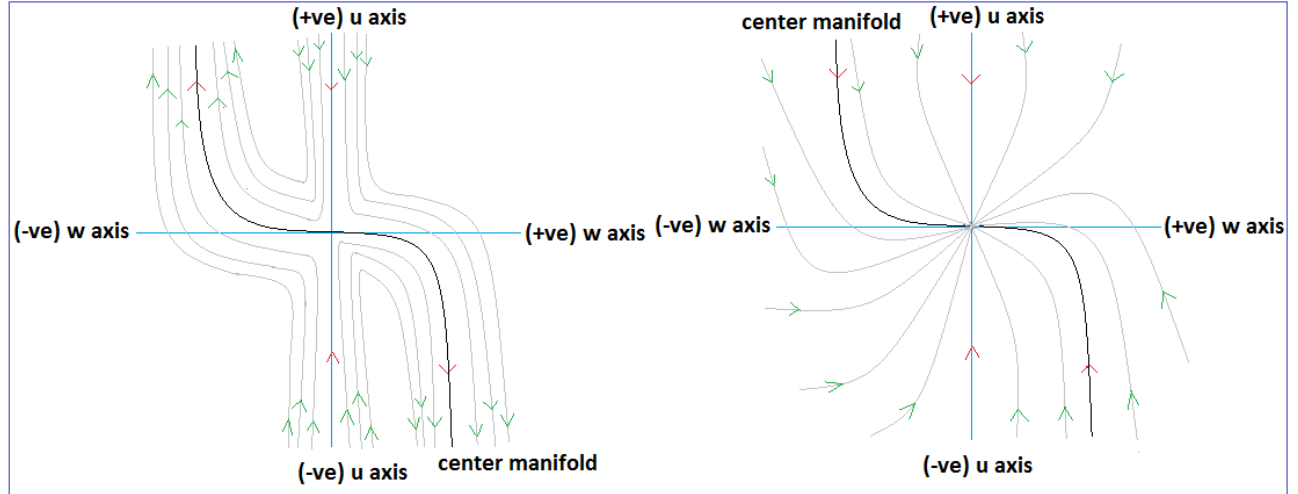


FIG. 4: Vector field near the origin for the Critical point A_3 in (uw) -plane. L.H.S. figure is for $\lambda > 0$ and R.H.S. figure is for $\lambda < 0$.

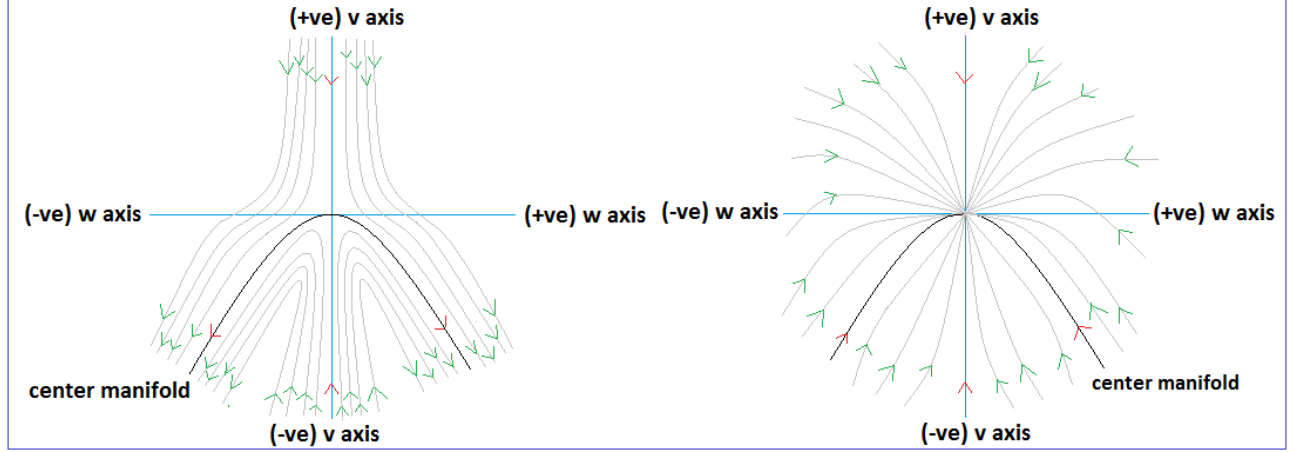


FIG. 5: Vector field near the origin for the Critical point A_3 in (vw) -plane. L.H.S. figure is for $\lambda > 0$ and R.H.S. figure is for $\lambda < 0$.

Case-(ii) $\mu \neq 0$ and $\lambda = 0$

In this case the autonomous system (22 – 24) changes into

$$x' = -3x + \frac{3}{2}x(1 - x^2 - y^2) - \frac{\mu}{2}z(1 + x^2 - y^2), \quad (46)$$

$$y' = \frac{3}{2}y(1 - x^2 - y^2), \quad (47)$$

$$z' = -xz^2. \quad (48)$$

We have also three critical points corresponding to the above autonomous system, in which two are space of critical points. The critical points for this autonomous system are $C_1(0, 0, 0)$, $C_2(0, 1, z_c)$ and $C_3(0, -1, z_c)$ where z_c is any real number. Corresponding to the critical points C_0 , C_1 and C_2 the eigenvalues of the Jacobian matrix, value of cosmological parameters and the nature of the critical points are same as A_1 , A_2 and A_3 respectively.

1. Critical Point C_1

The Jacobian matrix $J(C_1)$ for the autonomous system (46 – 48) at this critical point is same as (25). So, all the eigenvalues and the corresponding eigenvectors are also same as for $J(C_1)$. If we put forward argument like the stability analysis of the critical point A_1 then the center manifold can be expressed as (31 – 32) and the flow on the center manifold is determined by (33). So the stability of the vector field near the origin is same as for the critical point A_1 .

2. Critical Point C_2

The Jacobian matrix at the critical point C_2 can be put as

$$J(C_2) = \begin{bmatrix} -3 & \mu z_c & 0 \\ 0 & -3 & 0 \\ -z_c^2 & 0 & 0 \end{bmatrix}. \quad (49)$$

The eigenvalues of the above matrix are $-3, -3, 0$. $[1, 0, \frac{z_c^2}{3}]^T$ and $[0, 1, 0]^T$ are the eigenvectors corresponding to the eigenvalue -3 and $[0, 0, 1]^T$ be the eigenvector corresponding to the eigenvalue 0 . To apply CMT for a fixed z_c , first we transform the coordinates into a new system $x = X$, $y = Y + 1$, $z = Z + z_c$, such that the critical point is at the origin and after that if we put forward argument as above to determine center manifold, then the center manifold can be written as

$$X = 0, \quad (50)$$

$$Y = 0 \quad (51)$$

and the flow on the center manifold is determined by

$$Z' = 0. \quad (52)$$

So, the center manifold is lying on the Z -axis and the flow on the center manifold can not be determined by (52). Now, if we project the vector field on the plane which is parallel to XY -plane, i.e., the plane $Z = \text{constant}$ (say), then the vector field is shown as in FIG.6. So every point on Z - axis is a stable star.

2. Critical Point C_3

If we put forward argument as above to obtain the center manifold and the flow on the center manifold. Then we will get the center manifold same as (50 – 51) and the flow on the center manifold is determined by (52). In this case also we will get the same vector field as FIG.6.

From the above discussion, firstly we have seen that the space of critical points C_2 and C_3 are non-hyperbolic in nature but by using CMT we could not determine the vector field near those critical points and also the flow on the vector field. So, in this case the last eqn.(48) of the autonomous system (46 – 48) did not provide any special behaviour. For this reason and as the expressions of Ω_ϕ , ω_ϕ and ω_{total} depends only on x and y coordinates, we want to take only the first two equations of the autonomous system (46 – 48) and try to analyze the stability of the critical points which are lying on the plane, parallel to xy -plane, i.e., the plane $z = \text{constant} = c$ (say). In $z = c$ plane the first two equations in (46 – 48) can be written as

$$x' = -3x + \frac{3}{2}x(1 - x^2 - y^2) - \frac{\mu}{2}c(1 + x^2 - y^2), \quad (53)$$

$$y' = \frac{3}{2}y(1 - x^2 - y^2). \quad (54)$$

In this case we have five critical points corresponding to the autonomous system (53 – 54). The set of critical points, existence of critical points and the value of cosmological parameters are shown in Table II and the eigenvalues and the nature of critical points are shown in Table III.

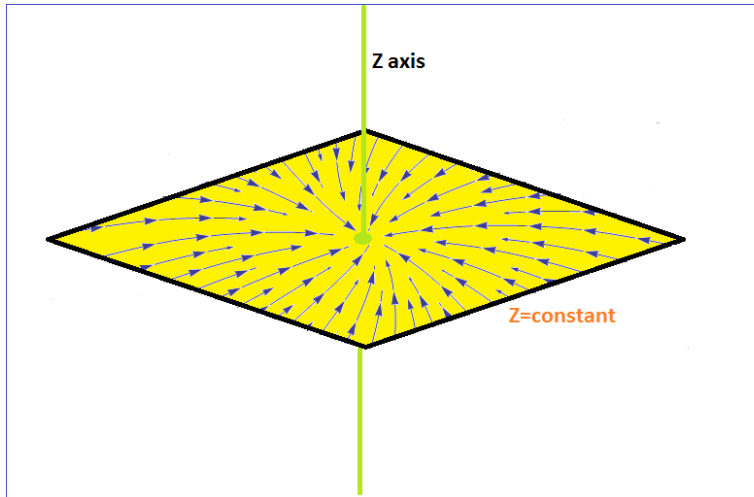


FIG. 6: Vector field near about every point on Z -axis for the critical points C_2 and C_3 .

TABLE II: Table shows the set of critical points, existence of critical points and the value of cosmological parameters corresponding to the autonomous system (53 – 54).

CP_s	<i>Existence</i>	x	y	Ω_ϕ	ω_ϕ	ω_{tot}	q
E_1	<i>For all μ and c</i>	0	1	1	-1	-1	-1
E_2	<i>For all μ and c</i>	0	-1	1	-1	-1	-1
E_3	<i>For all μ and c</i>	$-\frac{\mu c}{3}$	0	$-\frac{\mu^2 c^2}{9}$	-1	$-\frac{\mu^2 c^2}{9}$	$\frac{1}{2} \left(1 - \frac{\mu^2 c^2}{3}\right)$
E_4	<i>For $c \neq 0$ and for all $\mu \in (-\infty, -\frac{3}{c}] \cup [\frac{3}{c}, \infty)$</i>	$-\frac{3}{\mu c}$	$\sqrt{1 - \frac{9}{\mu^2 c^2}}$	$\left(1 - \frac{18}{\mu^2 c^2}\right)$	$\frac{\mu^2 c^2}{18 - \mu^2 c^2}$	-1	-1
E_5	<i>For $c \neq 0$ and for all $\mu \in (-\infty, -\frac{3}{c}] \cup [\frac{3}{c}, \infty)$</i>	$-\frac{3}{\mu c}$	$-\sqrt{1 - \frac{9}{\mu^2 c^2}}$	$\left(1 - \frac{18}{\mu^2 c^2}\right)$	$\frac{\mu^2 c^2}{18 - \mu^2 c^2}$	-1	-1

TABLE III: Table shows the eigenvalues (λ_1, λ_2) of the Jacobian matrix corresponding to the critical points and the nature of all critical points ($E_1 - E_5$).

<i>Critical Points</i>	λ_1	λ_2	<i>Nature of Critical points</i>
E_1	-3	-3	Hyperbolic
E_2	-3	-3	Hyperbolic
E_3	$-\frac{3}{2} \left(1 + \frac{\mu^2 c^2}{9}\right)$	$\frac{3}{2} \left(1 - \frac{\mu^2 c^2}{9}\right)$	Non-hyperbolic for $\mu c = \pm 3$ and hyperbolic for $\mu c \neq \pm 3$
E_4	$\frac{-3 + \sqrt{45 - \frac{324}{\mu^2 c^2}}}{2}$	$\frac{-3 - \sqrt{45 - \frac{324}{\mu^2 c^2}}}{2}$	Non-hyperbolic for $\mu c = \pm 3$ and hyperbolic for $\mu c \neq \pm 3$
E_5	$\frac{-3 + \sqrt{45 - \frac{324}{\mu^2 c^2}}}{2}$	$\frac{-3 - \sqrt{45 - \frac{324}{\mu^2 c^2}}}{2}$	Non-hyperbolic for $\mu c = \pm 3$ and hyperbolic for $\mu c \neq \pm 3$

For avoiding similar arguments which we have mentioned for analyzing the stability of the above critical points, we only state the stability and the reason behind the stability of these critical points in a tabular form, which is shown as in Table IV. Note that $\mu c \geq 3$ and $\mu c \leq -3$ be the domain of existence of the critical point E_4 and E_5 . For this reason we did not determine the stability analysis of the critical points E_4 and E_5 for $\mu c \in (-3, 3)$.

TABLE IV: Table shows the stability and the reason behind the stability of the critical points ($E_1 - E_5$)

CPs	$Stability$	$Reason\ behind\ the\ stability$
E_1, E_2	Both are stable star	As both eigenvalues λ_1 and λ_2 are negative and equal. By Hartman-Grobman theorem we can conclude that the critical points E_1 and E_2 both are stable star.
E_3	Stable node for $\mu c = -3$, saddle node for $\mu c = 3$, stable node for $\mu c > 3$ or, < -3 , saddle node for $-3 < \mu c < 3$	<p>For $\mu c = -3$:</p> <p>After shifting the this critical point into the origin by taking the transformation $x = X - \frac{\mu c}{3}$, $y = Y$ and by using CMT, the CM is given by $X = Y^2 + \mathcal{O}(Y^4)$ and the flow on the CM is determined by $Y' = -\frac{3}{2}Y^3 + \mathcal{O}(Y^5)$. $Y' < 0$ while $Y > 0$ and for $Y < 0$, $Y' > 0$. So, the critical point E_3 is a stable node (FIG.7(a)).</p> <p>For $\mu c = 3$:</p> <p>The center manifold is given by $X = -Y^2 + \mathcal{O}(Y^4)$ and the flow on the center manifold is determined by $Y' = \frac{3}{2}Y^3 + \mathcal{O}(Y^5)$. $Y' < 0$ while $Y < 0$ and for $Y > 0$, $Y' > 0$. So, the critical point E_3 is a saddle node (FIG.7(b)).</p> <p>For $\mu c > 3$ or, $\mu c < -3$:</p> <p>Both of the eigenvalues λ_1 and λ_2 are negative and unequal. So by Hartman-Grobman theorem the critical point E_3 is a stable node.</p> <p>For $-3 < \mu c < 3$:</p> <p>λ_1 is negative and λ_2 is positive. So by Hartman-Grobman theorem the critical point E_3 is unstable node.</p>
E_4, E_5	Both are stable node for $\mu c = -3$, saddle node for $\mu c = 3$, stable node for $\mu c > 3$ or, < -3	<p>For $\mu c = 3$ and $\mu c = -3$:</p> <p>The expression of the center manifold and the flow on the center manifold is same as the expressions for $\mu c = -3$ and $\mu c = -3$ cases respectively for E_3.</p> <p>For $\mu c > 3$, or < -3:</p> <p>Both of the eigenvalues λ_1 and λ_2 are negative and unequal. Hence, by Hartman-Grobman theorem we can conclude that the critical points E_4 and E_5 both are unstable in nature.</p>

Case-(iii) $\mu = 0$ and $\lambda \neq 0$

In this case the autonomous system (22 – 24) changes into

$$x' = -3x + \frac{3}{2}x(1 - x^2 - y^2) - \frac{\lambda y^2 z}{2}, \quad (55)$$

$$y' = \frac{3}{2}y(1 - x^2 - y^2) - \frac{\lambda x y z}{2}, \quad (56)$$

$$z' = -x z^2. \quad (57)$$

Corresponding to the above autonomous system we have three space of critical points $P_1(0, 0, z_c)$, $P_2(0, 1, 0)$ and $P_3(0, -1, 0)$ where z_c is any real number. The value of cosmological parameters, eigenvalues of the Jacobian matrix at those critical points corresponding to the autonomous system (55 – 57) and the nature of critical points P_1 , P_2 and P_3 are same as for the critical points A_1 , A_2 and A_3 respectively, shown as in Table I.

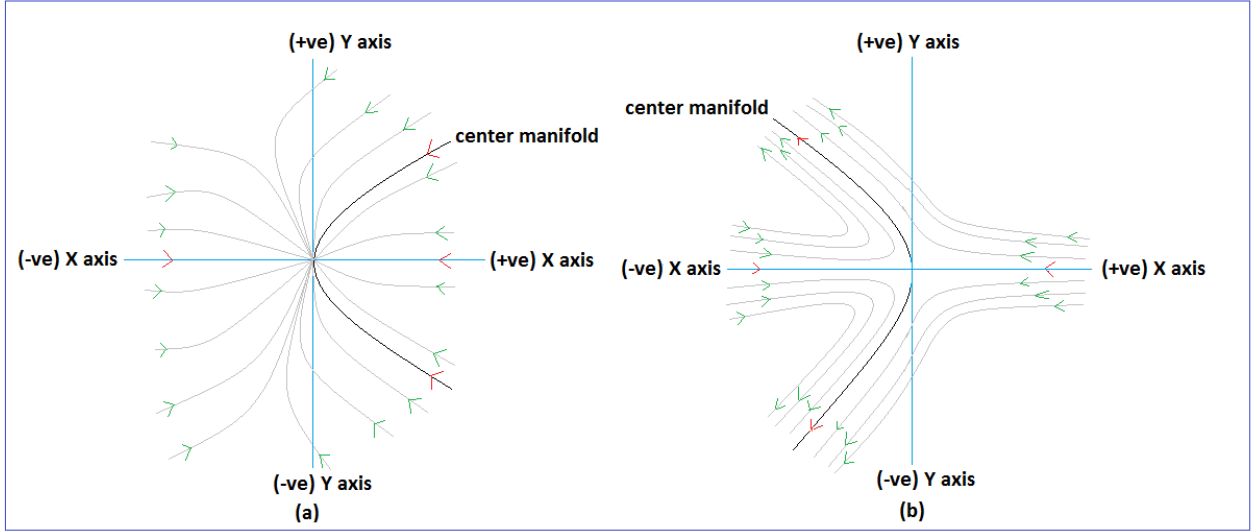


FIG. 7: Vector field near near the origin for the critical point E_3 . L.H.S. for $\mu c = 3$ and R.H.S. for $\mu c = -3$.

1. Critical Point P_1

The Jacobian matrix at the critical point P_1 can be put as

$$J(P_1) = \begin{bmatrix} -\frac{3}{2} & 0 & 0 \\ 0 & \frac{3}{2} & 0 \\ -z_c^2 & 0 & 0 \end{bmatrix}. \quad (58)$$

The eigenvalues of the above matrix are $-\frac{3}{2}$, $\frac{3}{2}$ and 0 and $[1, 0, \frac{2}{3}z_c^2]^T$, $[0, 1, 0]^T$ and $[0, 0, 1]^T$ are the corresponding eigenvectors respectively. For a fixed z_c , first we shift the critical point P_0 to the origin by the coordinate transformation $x = X$, $y = Y$ and $z = Z + z_c$, if we put forward argument as above for non-hyperbolic critical points. Then, the center manifold can be written as (50–51) and the flow on the center manifold is determined by (52). Similarly as above (the discussion of stability for the critical point C_2) we can conclude that the center manifold for the critical point P_1 is also lying in the Z -axis but flow on the center manifold can not be determined. Now, if we project the vector field on the plane which is parallel to XY -plane, i.e., the plane $Z = \text{constant}$ (say), then the vector field is shown as in FIG.8. So every point on Z - axis is a saddle node.

Again if we want to obtain the stability of the critical points in the plane which is parallel to xy -plane, i.e., $z = \text{constant} = c$ (say), then we only take the first two equations (55) and (56) of the autonomous system (55–57) and also replace z by c in those two equations. After that we can see that there exists three real and physically meaningful hyperbolic critical points $B_1(0,0)$, $B_2\left(-\frac{\lambda c}{6}, \sqrt{1 + \frac{\lambda^2 c^2}{36}}\right)$ and $B_3\left(-\frac{\lambda c}{6}, -\sqrt{1 + \frac{\lambda^2 c^2}{36}}\right)$. So by obtaining the eigenvalues of the Jacobian matrix corresponding to the autonomous system at those critical points and using Hartman-Grobman theorem we only state the stability of all critical points and also write the value of cosmological parameters corresponding to these critical points in tabular form, which is shown as in Table V.

For the critical points P_2 and P_3 we have the same Jacobian matrix (34) and if we will take the similar transformations (shifting and matrix) and then by using the similar arguments as A_2 and A_3 respectively, we conclude that the the stability of P_2 and P_3 is same as A_2 and A_3 respectively.

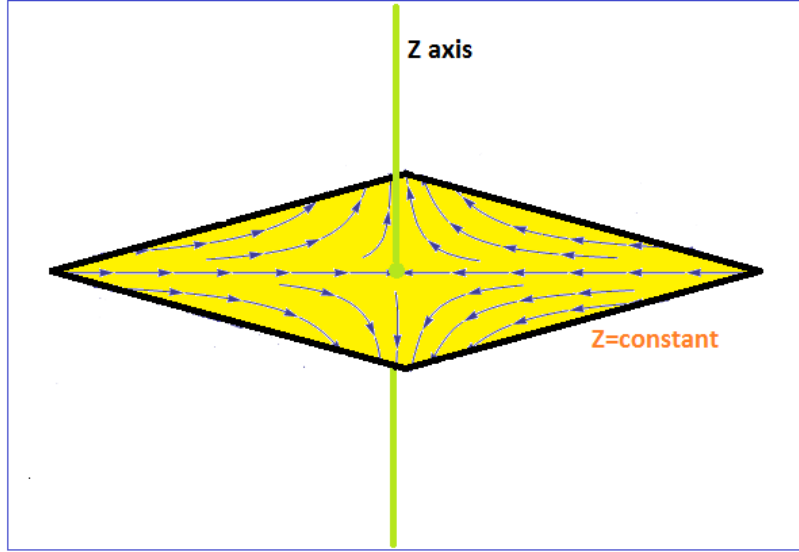


FIG. 8: Vector field near about every point on Z -axis for the critical point P_1 .

TABLE V: Table shows the eigenvalues (λ_1, λ_2) of the Jacobian matrix, stability and value of cosmological parameters corresponding to the critical points and the nature of all critical points ($B_1 - B_3$).

Critical Points	λ_1	λ_2	Stability	Ω_ϕ	ω_ϕ	ω_{tot}	q
B_1	$-\frac{3}{2}$	$\frac{3}{2}$	Stable star	0	Undetermined	0	$\frac{1}{2}$
B_2, B_3	$-3\left(1 + \frac{\lambda^2 c^2}{18}\right)$	$-3\left(1 + \frac{\lambda^2 c^2}{36}\right)$	Stable star for $\lambda c = 0$ and stable node for $\lambda c \neq 0$	1	$-\left(1 + \frac{\lambda^2 c^2}{18}\right)$	$-\left(1 + \frac{\lambda^2 c^2}{18}\right)$	$-\left(1 + \frac{\lambda^2 c^2}{12}\right)$

Case-(iv) $\mu = 0$ and $\lambda = 0$

In this case the autonomous system (22 – 24) changes into

$$x' = -3x + \frac{3}{2}x(1 - x^2 - y^2), \quad (59)$$

$$y' = \frac{3}{2}y(1 - x^2 - y^2), \quad (60)$$

$$z' = -xz^2. \quad (61)$$

Corresponding to the above autonomous system we have three space of critical points $S_1(0, 0, z_c)$, $S_2(0, 1, z_c)$ and $S_3(0, -1, z_c)$ where z_c is any real number, which are exactly same as C_1, C_2 and C_3 . In this case also all critical points are non-hyperbolic in nature. By taking the possible shifting transformations (for S_1 ($x = X, y = Y, z = Z + z_c$), for S_2 ($x = X, y = Y + 1, z = Z + z_c$) and for S_3 ($x = X, y = Y - 1, z = Z + z_c$)) as above we can conclude that for all critical points the center manifold is given by (50 – 51) and the flow on the center manifold is determined by (52), i.e., for all critical points the center manifold is lying on the Z -axis. Again if we plot the vector field in $Z = \text{constant}$ plane, we can see that for the critical point S_1 every points on Z -axis is a saddle node (same as FIG.8) and for S_2 and S_3 every points on Z -axis is a stable star (same as FIG.6).

B. Model 2: Power-law potential and exponentially-dependent dark-matter particle mass

In this consideration evolution equations in Section II can be converted to the autonomous system as follows

$$x' = -3x + \frac{3}{2}x(1 - x^2 - y^2) - \frac{\lambda y^2 z}{2} - \sqrt{\frac{3}{2}}\mu(1 + x^2 - y^2), \quad (62)$$

$$y' = \frac{3}{2}y(1 - x^2 - y^2) - \frac{\lambda xyz}{2}, \quad (63)$$

$$z' = -xz^2, \quad (64)$$

We have five critical points L_1, L_2, L_3, L_4 and L_5 corresponding to the above autonomous system. The set of critical points, their existence and the value of cosmological parameters at those critical points are shown as in Table VI and the eigenvalues of the Jacobian matrix corresponding to the autonomous system (62 – 64) at those critical points and the nature of the critical points are shown in Table VII.

Here we only concern about the stability of the critical points for $\mu \neq 0$ and $\lambda \neq 0$ because for another possible cases we will get the similar types result which we have obtained for Model 1.

TABLE VI: Table shows the set of critical points and their existence, value of cosmological parameters corresponding to that critical points.

Critical Points	Existence	x	y	z	Ω_ϕ	ω_ϕ	ω_{tot}	q
L_1	For all μ and λ	0	1	0	1	-1	-1	-1
L_2	For all μ and λ	0	-1	0	1	-1	-1	-1
L_3	For all $\mu \in \left(-\infty, -\sqrt{\frac{3}{2}}\right] \cup \left[\sqrt{\frac{3}{2}}, \infty\right)$ and all λ	$-\frac{1}{\mu}\sqrt{\frac{3}{2}}$	$\sqrt{1 - \frac{3}{2\mu^2}}$	0	$1 - \frac{3}{\mu^2}$	$\frac{\mu^2}{3 - \mu^2}$	-1	-1
L_4	For all $\mu \in \left(-\infty, -\sqrt{\frac{3}{2}}\right] \cup \left[\sqrt{\frac{3}{2}}, \infty\right)$ and all λ	$-\frac{1}{\mu}\sqrt{\frac{3}{2}}$	$-\sqrt{1 - \frac{3}{2\mu^2}}$	0	$1 - \frac{3}{\mu^2}$	$\frac{\mu^2}{3 - \mu^2}$	-1	-1
L_5	For all μ and λ	$-\sqrt{\frac{2}{3}}\mu$	0	0	$-\frac{2}{3}\mu^2$	1	$-\frac{2}{3}\mu^2$	$\frac{1}{2}(1 - 2\mu^2)$

1. Critical Point L_1

The Jacobian matrix corresponding to the autonomous system (62 – 64) at the critical point L_1 can be put as

$$J(L_1) = \begin{bmatrix} -3 & \sqrt{6}\mu & -\frac{\lambda}{2} \\ 0 & -3 & 0 \\ 0 & 0 & 0 \end{bmatrix}. \quad (65)$$

The eigenvalues of $J(L_1)$ are $-3, -3, 0$ and $[1, 0, 0]^T, [-\frac{\lambda}{6}, 0, 1]^T$ are the eigenvectors corresponding to the eigenvalues -3 and 0 respectively. Since the algebraic multiplicity corresponding to the eigenvalue -3 is 2 but the dimension of the eigenspace corresponding to that eigenvalue is 1, i.e., algebraic multiplicity and geometric multiplicity corresponding to the eigenvalue -3 are not equal to each other. So, the Jacobian matrix $J(L_1)$ is not diagonalizable. To determine the center manifold for this critical point there only arises a problem for presence of the nonzero element in the top position of third column of the Jacobian matrix. First we take the

TABLE VII: The eigenvalues ($\lambda_1, \lambda_2, \lambda_3$) of the Jacobian matrix corresponding to the autonomous system (62–64) at those critical points ($L_1 - L_5$) and the nature of the critical points

Critical Points	λ_1	λ_2	λ_3	Nature of critical Points
L_1	-3	-3	0	Non-hyperbolic
L_2	-3	-3	0	Non-hyperbolic
L_3	$-\frac{3}{2} \left(1 + \frac{1}{\mu} \sqrt{-6 + 5\mu^2}\right)$	$-\frac{3}{2} \left(1 - \frac{1}{\mu} \sqrt{-6 + 5\mu^2}\right)$	0	Non-hyperbolic
L_4	$-\frac{3}{2} \left(1 + \frac{1}{\mu} \sqrt{-6 + 5\mu^2}\right)$	$-\frac{3}{2} \left(1 - \frac{1}{\mu} \sqrt{-6 + 5\mu^2}\right)$	0	Non-hyperbolic
L_5	$-\frac{3}{2}$	$\frac{3}{2}$	0	Non-hyperbolic

coordinate transformation $x = X, y = Y + 1, z = Z$ which shift the critical point L_1 to the origin. Now we introduce another coordinate system which will remove the term in the top position of the third column. Since, there are only two linearly independent eigenvectors, so we have to obtain another linearly independent column vector that will help to construct the new coordinate system. Since, $[0, 1, 0]^T$ be the column vector which is linearly independent to the eigenvectors of $J(L_1)$. The new coordinate system (u, v, w) can be written in terms of (X, Y, Z) as (35) and in these new coordinate system the equations (62–64) are transformed into

$$\begin{bmatrix} u' \\ v' \\ w' \end{bmatrix} = \begin{bmatrix} -3 & \sqrt{6}\mu & 0 \\ 0 & -3 & 0 \\ 0 & 0 & 0 \end{bmatrix} \begin{bmatrix} u \\ v \\ w \end{bmatrix} + \begin{bmatrix} \text{non} \\ \text{linear} \\ \text{terms} \end{bmatrix}. \quad (66)$$

By similar arguments which we have derived in the stability analysis of the critical point A_2 , the center manifold can be written as (40-41) and the flow on the center manifold is determined by (42). As the expression of center manifold and the flow are same as for the critical point A_2 . So the stability of the critical point L_1 is same as the stability of A_2 .

2. Critical Point L_2

After shifting the critical points to the origin (by taking the shifting transformations ($x = X, y = Y - 1, z = Z$) and the matrix transformation (35)) and by putting the forward arguments which we have mentioned for the analysis of L_1 , the center manifold can be expressed as (43–44) and the flow on the center manifold is determined by (45). So the stability of the critical point L_2 is same as the stability of A_3 .

3. Critical Point L_3

The Jacobian matrix corresponding to the autonomous system (62–64) at the critical point L_3 can be put as

$$J(L_3) = \begin{bmatrix} -\frac{9}{2\mu^2} & \sqrt{1 - \frac{3}{2\mu^2}} \left(\frac{3}{\mu} \sqrt{\frac{3}{2}} + \sqrt{6}\mu \right) & -\frac{\lambda}{2} \left(1 - \frac{3}{2\mu^2} \right) \\ \frac{3}{\mu} \sqrt{\frac{3}{2}} \sqrt{1 - \frac{3}{2\mu^2}} & -3 \left(1 - \frac{3}{2\mu^2} \right) & \frac{\lambda}{2\mu} \sqrt{\frac{3}{2}} \sqrt{1 - \frac{3}{2\mu^2}} \\ 0 & 0 & 0 \end{bmatrix}. \quad (67)$$

The eigenvalues corresponding to the Jacobian matrix $J(L_3)$ are shown in Table.VII. From the existence of the critical point L_3 we can conclude that the eigenvalues of $J(L_3)$ always real. Since the critical point L_3 exists

for $\mu \leq -\sqrt{\frac{3}{2}}$ or $\mu \geq \sqrt{\frac{3}{2}}$, our aim is to define the stability in all possible regions of μ for at least one choice of μ in these region. For this reason we will define the stability at four possible choices of μ . We first determine the stability of this critical point at $\mu = \pm\sqrt{\frac{3}{2}}$. Then for $\mu < -\sqrt{\frac{3}{2}}$, we shall determine the stability of L_3 at $\mu = -\sqrt{3}$ and for $\mu > \sqrt{\frac{3}{2}}$, we shall determine the stability of L_3 at $\mu = \sqrt{3}$.

For $\mu = \pm\sqrt{\frac{3}{2}}$, the Jacobian matrix $J(L_3)$ converts into

$$\begin{bmatrix} -3 & 0 & 0 \\ 0 & 0 & 0 \\ 0 & 0 & 0 \end{bmatrix}$$

and as the critical point L_3 converts into $(\mp 1, 0, 0)$, first we take the transformation $x = X \mp 1, y = Y, z = Z$ so that L_3 moves into the origin. As the critical point is non-hyperbolic in nature we use CMT for determining the stability of this critical point. From center manifold theory there exist a continuously differentiable function $h : \mathbb{R}^2 \rightarrow \mathbb{R}$ such that $X = h(Y, Z) = aY^2 + bYZ + cZ^2 + \text{higher order terms}$, where $a, b, c \in \mathbb{R}$. Now differentiating both side with respect to N , we get

$$\frac{dX}{dN} = [2aY + bZ \quad bY + 2cZ] \begin{bmatrix} \frac{dY}{dN} \\ \frac{dZ}{dN} \end{bmatrix} \quad (68)$$

Comparing L.H.S. and R.H.S. of (68) we get, $a = 1, b = 0$ and $c = 0$, i.e., the center manifold can be written as

$$X = \pm Y^2 + \text{higher order terms} \quad (69)$$

and the flow on the center manifold is determined by

$$\frac{dY}{dN} = \pm \frac{\lambda}{2} YZ + \text{higher order terms}, \quad (70)$$

$$\frac{dZ}{dN} = \pm Z^2 + \text{higher order terms}. \quad (71)$$

We only concern about the non-zero coefficients of the lowest power terms in CMT as we analyze arbitrary small neighborhood of the origin and here the lowest power term of the expression of center manifold depends only on Y . So, we draw the vector field near the origin only on XY -plane, i.e., the nature of the vector field implicitly depends on Z not explicitly. Now we try to write the flow equations (70 – 71) in terms of Y only. For this reason, we divide the corresponding sides of (70) by the corresponding sides of (71) and then we will get

$$\begin{aligned} \frac{dY}{dZ} &= \frac{\lambda Y}{2 Z} \\ \implies Z &= \left(\frac{Y}{C}\right)^{2/\lambda}, \quad \text{where } C \text{ is a positive arbitrary constant} \end{aligned}$$

After substituting this any of (70) or (71), we get

$$\frac{dY}{dN} = \frac{\lambda}{2C^{2/\lambda}} Y^{1+2/\lambda} \quad (72)$$

As the power of Y can not be negative or fraction, so we have only two choices of λ , $\lambda = 1$ or $\lambda = 2$. For $\lambda = 1$ or, $\lambda = 2$ both of the cases the origin is a saddle node, i.e., unstable in nature (FIG.9 is for $\mu = \sqrt{\frac{3}{2}}$ and FIG.10 is for $\mu = -\sqrt{\frac{3}{2}}$). Hence, for $\mu = \pm\sqrt{\frac{3}{2}}$, in the old coordinate system the critical point L_3 is unstable due to its saddle nature.

For $\mu = \sqrt{3}$, the Jacobian matrix $J(L_3)$ converts into

$$\begin{bmatrix} -\frac{3}{2} & \frac{9}{2} & -\frac{\lambda}{4} \\ \frac{3}{2} & -\frac{3}{2} & \frac{\lambda}{4} \\ 0 & 0 & 0 \end{bmatrix}.$$

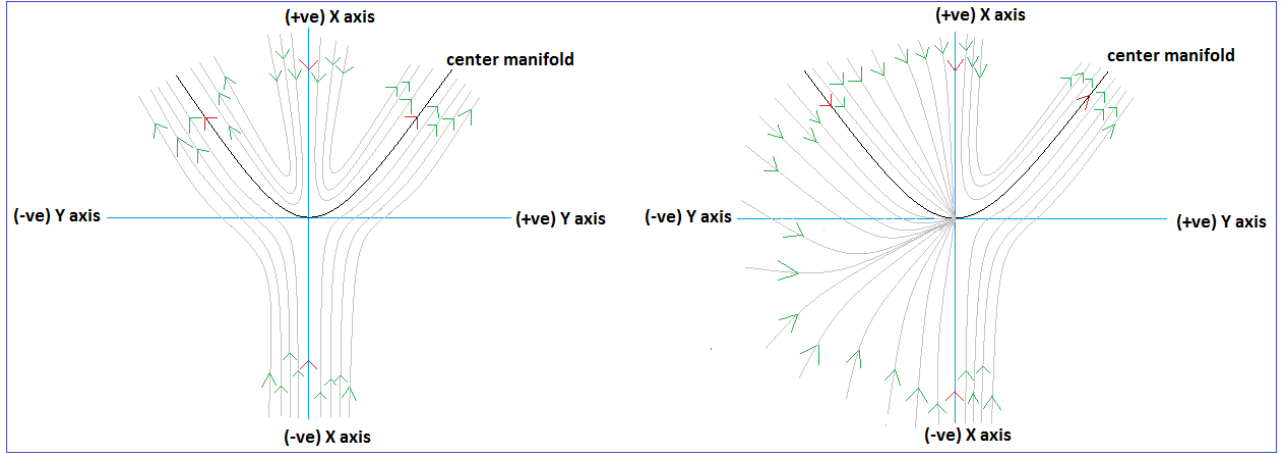


FIG. 9: Vector field near the origin when $\mu = \sqrt{\frac{3}{2}}$, for the critical point L_3 . L.H.S. phase plot is for $\lambda = 1$ and R.H.S. phase plot is for $\lambda = 2$.

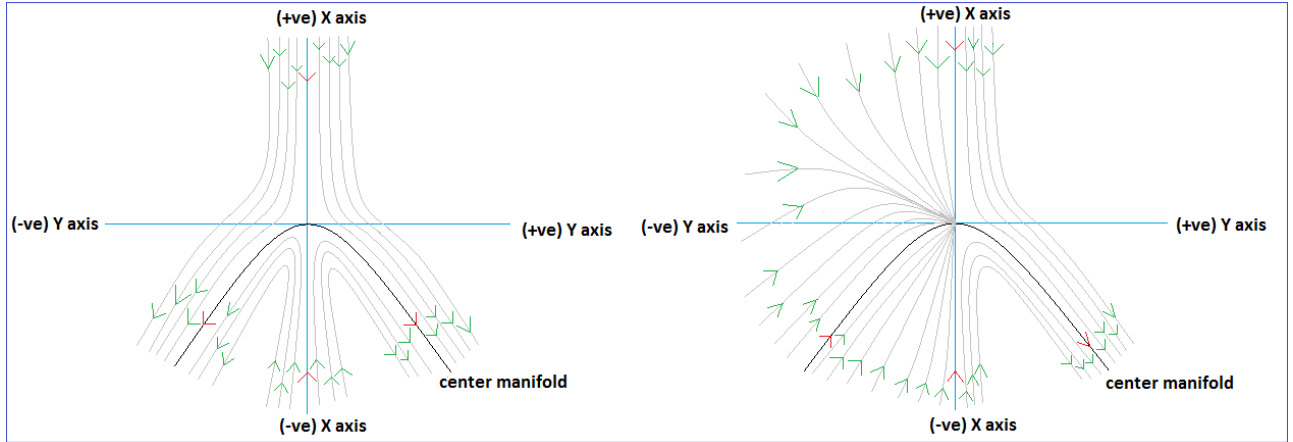


FIG. 10: Vector field near the origin when $\mu = -\sqrt{\frac{3}{2}}$, for the critical point L_3 . L.H.S. phase plot is for $\lambda = 1$ and R.H.S. phase plot is for $\lambda = 2$.

The eigenvalues of the above Jacobian matrix are $-\frac{3}{2}(1 + \sqrt{3})$, $-\frac{3}{2}(1 - \sqrt{3})$ and 0 and the corresponding eigenvectors are $[-\sqrt{3}, 1, 0]^T$, $[\sqrt{3}, 1, 0]^T$ and $[-\frac{\lambda}{6}, 0, 1]^T$ respectively. As for $\mu = \sqrt{3}$, the critical point L_3 converts into $(-\frac{1}{\sqrt{2}}, \frac{1}{\sqrt{2}}, 0)$; so first we take the transformations $x = X - \frac{1}{\sqrt{2}}$, $y = Y + \frac{1}{\sqrt{2}}$ and $z = Z$ which shift the critical point to the origin. By using the eigenvectors of the above Jacobian matrix, we introduce a new coordinate system (u, v, w) in terms of (X, Y, Z) as

$$\begin{bmatrix} u \\ v \\ w \end{bmatrix} = \begin{bmatrix} -\frac{1}{2\sqrt{3}} & \frac{1}{2} & -\frac{\lambda}{12\sqrt{3}} \\ \frac{1}{2\sqrt{3}} & \frac{1}{2} & \frac{\lambda}{12\sqrt{3}} \\ 0 & 0 & 1 \end{bmatrix} \begin{bmatrix} X \\ Y \\ Z \end{bmatrix} \quad (73)$$

and in these new coordinates the equations (62 – 64) are transformed into

$$\begin{bmatrix} -u' + v' \\ u' + v' \\ w' \end{bmatrix} = \begin{bmatrix} \frac{3}{2}(1 + \sqrt{3}) & -\frac{3}{2}(1 - \sqrt{3}) & 0 \\ -\frac{3}{2}(1 + \sqrt{3}) & -\frac{3}{2}(1 - \sqrt{3}) & 0 \\ 0 & 0 & 0 \end{bmatrix} \begin{bmatrix} u \\ v \\ w \end{bmatrix} + \begin{bmatrix} \text{non} \\ \text{linear} \\ \text{terms} \end{bmatrix}. \quad (74)$$

Now if we add 1st and 2nd equation of the above matrix equation and then divide both sides by 2, then we get v' . Again, if we subtract 1st equation from 2nd equation and divide both sides by 2, we get u' . Finally, in

matrix form in the new coordinate system the autonomous system can be written as

$$\begin{bmatrix} u' \\ v' \\ w' \end{bmatrix} = \begin{bmatrix} -\frac{3}{2}(1 + \sqrt{3}) & 0 & 0 \\ 0 & -\frac{3}{2}(1 - \sqrt{3}) & 0 \\ 0 & 0 & 0 \end{bmatrix} \begin{bmatrix} u \\ v \\ w \end{bmatrix} + \begin{bmatrix} \text{non} \\ \text{linear} \\ \text{terms} \end{bmatrix}. \quad (75)$$

If we put similar arguments which we have mentioned for the analysis of A_2 , then the center manifold can be expressed as

$$u = \frac{2}{3(1 + \sqrt{3})} \left\{ \frac{(\sqrt{3} - 1)\lambda^2 - 4\lambda}{48\sqrt{6}} \right\} w^2 + \mathcal{O}(w^3), \quad (76)$$

$$v = -\frac{2}{3(\sqrt{3} - 1)} \left\{ \frac{(\sqrt{3} + 1)\lambda^2 + 4\lambda}{48\sqrt{6}} \right\} w^2 + \mathcal{O}(w^3) \quad (77)$$

and the flow on the center manifold is determined by

$$w' = \frac{1}{\sqrt{2}} w^2 + \mathcal{O}(w^3). \quad (78)$$

From the flow equation we can easily conclude that the origin is a saddle node and unstable in nature. The vector field near the origin in uw -plane is shown as in FIG.11 and the vector field near the origin in vw -plane is shown as in FIG.12. Hence, in the old coordinate system (x, y, z) , for $\mu = \sqrt{3}$ the critical point L_3 is unstable due to its saddle nature.

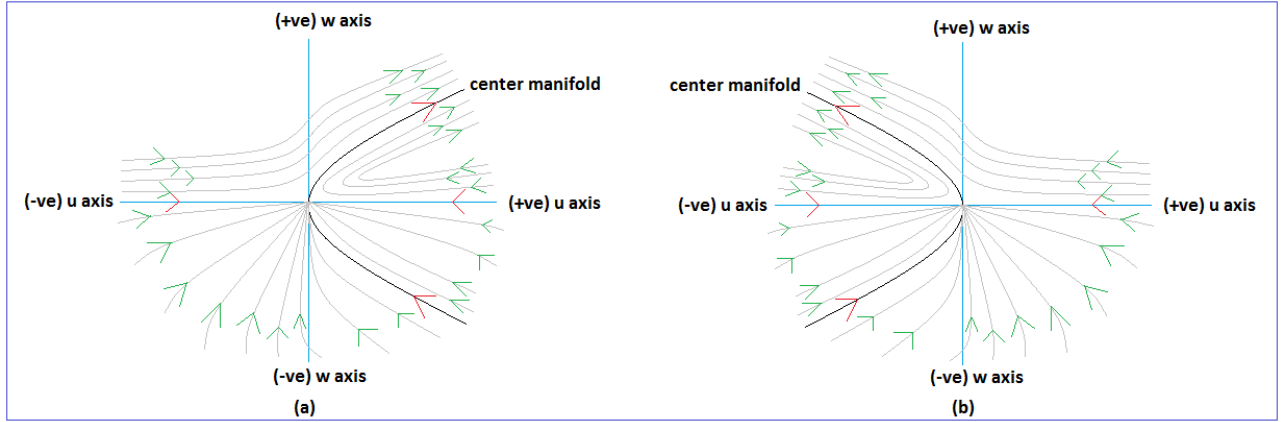


FIG. 11: Vector field near the origin in uw -plane when $\mu = \sqrt{3}$, for the critical points L_3 and L_4 . For the critical point L_3 , the phase plot (a) is for $\lambda < 0$ or $\lambda > \frac{4}{\sqrt{3}-1}$ and the phase plot (b) is for $0 < \lambda < \frac{4}{\sqrt{3}-1}$. For the critical point L_4 , the phase plot (a) is for $0 < \lambda < \frac{4}{\sqrt{3}-1}$ and the phase plot (b) is for $\lambda < 0$ or $\lambda > \frac{4}{\sqrt{3}-1}$.

Lastly, for $\mu = -\sqrt{3}$, we have the same eigenvalues $-\frac{3}{2}(1 + \sqrt{3})$, $-\frac{3}{2}(1 - \sqrt{3})$ and 0 and the corresponding eigenvectors are $[\sqrt{3}, 1, 0]^T$, $[-\sqrt{3}, 1, 0]^T$ and $[-\frac{\lambda}{6}, 0, 1]^T$ respectively of $J(L_3)$. After putting corresponding arguments which we have mentioned for $\mu = \sqrt{3}$ case, then we will get the same expressions (76 – 77) for center manifold and (78) for flow on the center manifold. So, for this case also we conclude that the critical point L_3 is a saddle node and unstable in nature.

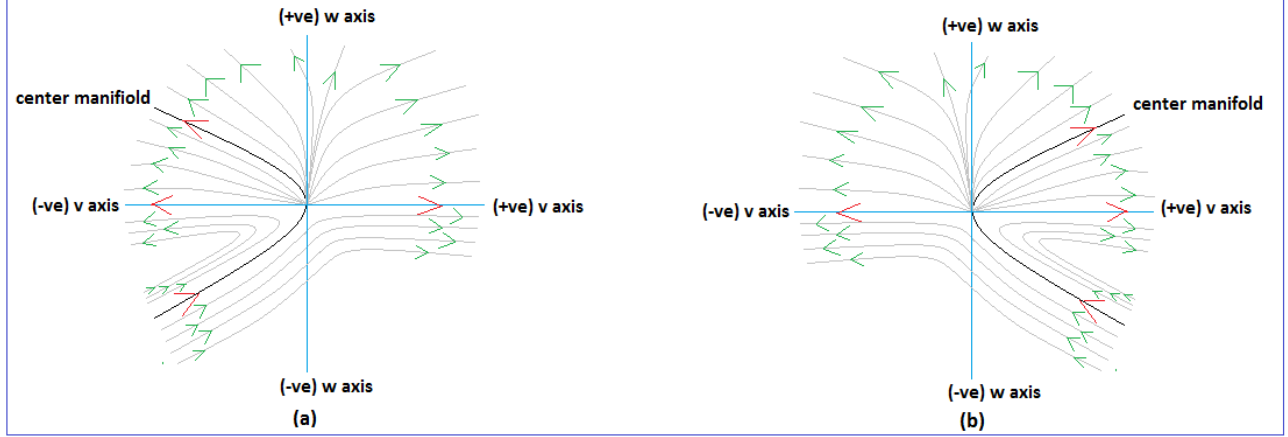


FIG. 12: Vector field near the origin in vw -plane when $\mu = \sqrt{3}$, for the critical points L_3 and L_4 . For the critical point L_3 , the phase plot (a) is for $\lambda < -\frac{4}{\sqrt{3}+1}$ or $\lambda > 0$ and the phase plot (b) is for $-\frac{4}{\sqrt{3}+1} < \lambda < 0$. For the critical point L_4 , the phase plot (a) is for $-\frac{4}{\sqrt{3}+1} < \lambda < 0$ and the phase plot (b) is for $\lambda < -\frac{4}{\sqrt{3}+1}$ or $\lambda > 0$.

4. Critical Point L_4

The Jacobian matrix corresponding to the autonomous system (62 – 64) at the critical point L_4 can be put as

$$J(L_4) = \begin{bmatrix} -\frac{9}{2\mu^2} & -\sqrt{1 - \frac{3}{2\mu^2}} \left(\frac{3}{\mu} \sqrt{\frac{3}{2}} + \sqrt{6}\mu \right) & -\frac{\lambda}{2} \left(1 - \frac{3}{2\mu^2} \right) \\ -\frac{3}{\mu} \sqrt{\frac{3}{2}} \sqrt{1 - \frac{3}{2\mu^2}} & -3 \left(1 - \frac{3}{2\mu^2} \right) & -\frac{\lambda}{2\mu} \sqrt{\frac{3}{2}} \sqrt{1 - \frac{3}{2\mu^2}} \\ 0 & 0 & 0 \end{bmatrix}. \quad (79)$$

For this critical point also we analyze the stability for the above four choices of μ , i.e., $\mu = \pm\sqrt{\frac{3}{2}}$, $\mu = \sqrt{3}$ and $\mu = -\sqrt{3}$.

For $\mu = \pm\sqrt{\frac{3}{2}}$, we will get the same expressions of center manifold (69) and the flow on the center manifold (70 – 71). So, for this case the critical point L_4 is unstable due to its saddle nature.

For $\mu = \sqrt{3}$, after putting corresponding arguments as L_3 , the center manifold can be written as

$$u = \frac{2}{3(1 + \sqrt{3})} \left\{ \frac{(1 - \sqrt{3})\lambda^2 + 4\lambda}{48\sqrt{6}} \right\} w^2 + \mathcal{O}(w^3), \quad (80)$$

$$v = \frac{2}{3(\sqrt{3} - 1)} \left\{ \frac{(\sqrt{3} + 1)\lambda^2 + 4\lambda}{48\sqrt{6}} \right\} w^2 + \mathcal{O}(w^3) \quad (81)$$

and the flow on the center manifold is determined by

$$w' = \frac{1}{\sqrt{2}} w^2 + \mathcal{O}(w^3). \quad (82)$$

From the flow equation we can conclude that the origin is a saddle node and hence in the old coordinate system L_4 is a saddle node, i.e., unstable in nature. The vector field near the origin in uw -plane is shown as in FIG.11 and the vector field near the origin in vw -plane is shown as in FIG.12.

For $\mu = -\sqrt{3}$ we also get the same expression of center manifold and flow equation as for $\mu = \sqrt{3}$ case.

5. Critical Point L_5

First we shift the critical point L_5 to the origin by the transformation $x = X - \sqrt{\frac{2}{3}}\mu$, $y = Y$ and $z = Z$. For avoiding similar arguments which we have mentioned for the above critical points, we only state the main results center manifold and the flow equation for this critical point. The center manifold for this critical point can be written as

$$X = 0, \quad (83)$$

$$Y = 0 \quad (84)$$

and the flow on the center manifold can be obtained as

$$\frac{dZ}{dN} = \sqrt{\frac{2}{3}}\mu Z^2 + \mathcal{O}(Z^3). \quad (85)$$

From the expressions of the center manifold we can conclude that the center manifold is lying on the Z -axis. From the flow on the center manifold FIG.13, we conclude that the origin is unstable for both of the cases $\mu > 0$ or $\mu < 0$.

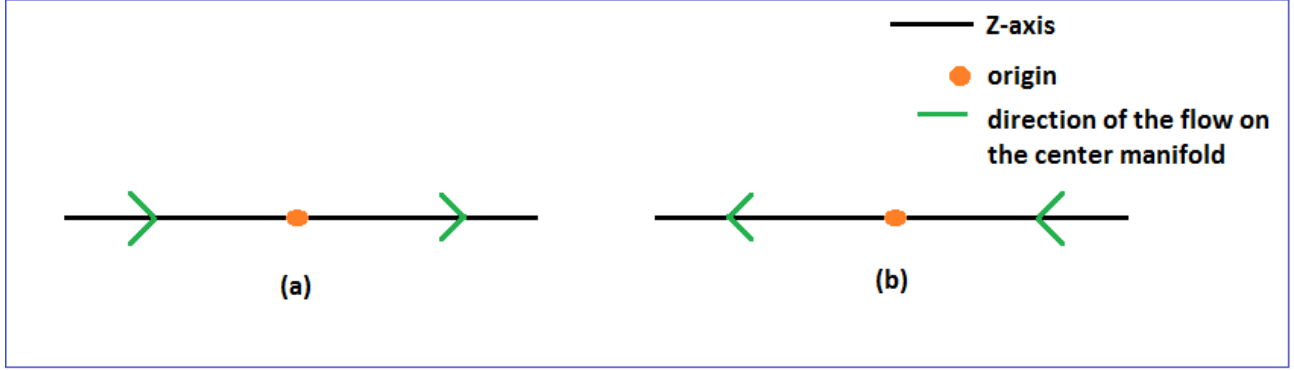


FIG. 13: Flow on the center manifold near the origin for the critical point L_5 . (a) is for $\mu > 0$ and (b) is for $\mu < 0$.

C. Model 3: Exponential potential and power-law-dependent dark-matter particle mass

In this case evolution equations in Section II can be written to the autonomous system as follows

$$x' = -3x + \frac{3}{2}x(1 - x^2 - y^2) - \sqrt{\frac{3}{2}}\lambda y^2 - \frac{\mu}{2}z(1 + x^2 - y^2), \quad (86)$$

$$y' = \frac{3}{2}y(1 - x^2 - y^2) - \sqrt{\frac{3}{2}}\lambda xy, \quad (87)$$

$$z' = -xz^2. \quad (88)$$

We have three physical meaningful critical points R_1 , R_2 and R_3 corresponding to the above autonomous system. The set of critical points, their existence and the value of cosmological parameters at those critical points corresponding to the autonomous system (86 – 88) shown in Table VIII and the eigenvalues of the Jacobian matrix corresponding to the autonomous system (86 – 88) at those critical points and the nature of the critical points are shown in Table IX.

Here we also concern about the stability of the critical points for $\mu \neq 0$ and $\lambda \neq 0$ because for another possible cases we will get the similar types result which we have obtained for Model 1.

For avoiding similar types of argument, we only state the stability of every critical points and the reason behind the stability in the tabular form, which is shown as in Table X.

TABLE VIII: Table shows the set of critical points and their existence, value of cosmological parameters corresponding to that critical points.

<i>Critical Points</i>	<i>Existence</i>	x	y	z	Ω_X	ω_X	ω_{tot}	q
R_1	For all μ and λ	0	0	0	0	Undetermined	0	$\frac{1}{2}$
R_2	For all μ and λ	$-\frac{\lambda}{\sqrt{6}}$	$\sqrt{1 + \frac{\lambda^2}{6}}$	0	1	$-1 - \frac{\lambda^2}{3}$	$-1 - \frac{\lambda^2}{3}$	$-\frac{1}{2}(2 + \lambda^2)$
R_3	For all μ and λ	$-\frac{\lambda}{\sqrt{6}}$	$-\sqrt{1 + \frac{\lambda^2}{6}}$	0	1	$-1 - \frac{\lambda^2}{3}$	$-1 - \frac{\lambda^2}{3}$	$-\frac{1}{2}(2 + \lambda^2)$

TABLE IX: The eigenvalues ($\lambda_1, \lambda_2, \lambda_3$) of the Jacobian matrix corresponding to the autonomous system (86 – 88) at those critical points ($R_1 - R_3$) and the nature of the critical points.

<i>Critical Points</i>	λ_1	λ_2	λ_3	<i>Nature of critical Points</i>
R_1	$-\frac{3}{2}$	$\frac{3}{2}$	0	Non-hyperbolic
R_2	$-(3 + \lambda^2) - \left(3 + \frac{\lambda^2}{2}\right)$	0	0	Non-hyperbolic
R_3	$-(3 + \lambda^2) - \left(3 + \frac{\lambda^2}{2}\right)$	0	0	Non-hyperbolic

TABLE X: Table shows the stability and the reason behind the stability of the critical points ($R_1 - R_3$).

<i>CPs</i>	<i>Stability</i>	<i>Reason behind the stability</i>
R_1	For $\mu > 0$, R_1 is a saddle node and for $\mu < 0$, R_1 is a stable node	After introducing the coordinate transformation (26), we will get the same expression of center manifold (31 – 32) and the flow on the center manifold is determined by (33)(FIG.1).
R_2, R_3	For $\lambda > 0$ or $\lambda < 0$, R_2 and R_3 both are unstable	After shifting R_2 and R_3 to the origin by using coordinate transformation $\left(x = X - \frac{\lambda}{\sqrt{6}}, y = Y + \sqrt{1 + \frac{\lambda^2}{6}}, z = Z\right)$ and $\left(x = X - \frac{\lambda}{\sqrt{6}}, y = Y - \sqrt{1 + \frac{\lambda^2}{6}}, z = Z\right)$ respectively, we can conclude that the center manifold is lying on Z -axis and the flow on the center manifold is determined by $\frac{dZ}{dN} = \frac{\lambda}{\sqrt{6}}Z^2 + \mathcal{O}(Z^3)$. The origin is unstable for both of the cases $\lambda > 0$ (same as FIG.13(a)) and $\lambda < 0$ (same as FIG.13(b)).

D. Model 4: Exponential potential and exponentially-dependent dark-matter particle mass

In this consideration evolution equations in Section II can be written to the autonomous system as follows

$$x' = -3x + \frac{3}{2}x(1 - x^2 - y^2) - \sqrt{\frac{3}{2}}\lambda y^2 - \sqrt{\frac{3}{2}}\mu(1 + x^2 - y^2), \quad (89)$$

$$y' = \frac{3}{2}y(1 - x^2 - y^2) - \sqrt{\frac{3}{2}}\lambda xy. \quad (90)$$

We ignore the equation corresponding to the auxiliary variable z in the above autonomous system because the R.H.S. expression of x' and y' does not depend on z .

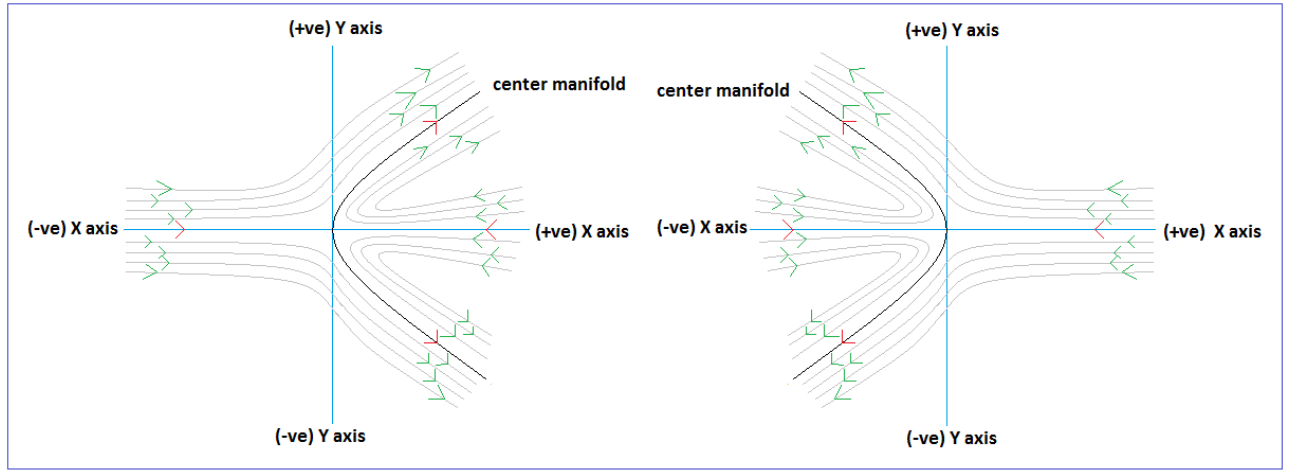


FIG. 14: Vector field near the origin for the critical point M_1 . L.H.S. for $\mu > 3$ and R.H.S. for $\mu < 0$.

Corresponding to the above autonomous system we have four critical points M_1 , M_2 , M_3 and M_4 . The set of critical points, their existence and the value of cosmological parameters at those critical points corresponding to the autonomous system (89 – 90) shown in Table XI and the eigenvalues of the Jacobian matrix corresponding to the autonomous system (89 – 90) at those critical points and the nature of the critical points are shown in Table XII.

TABLE XI: Table shows the set of critical points and their existence, value of cosmological parameters corresponding to that critical points.

<i>Critical Points</i>	<i>Existence</i>	x	y	Ω_X	ω_X	ω_{tot}	q
M_1	For all μ and λ	$-\sqrt{\frac{2}{3}}\mu$	0	$-\frac{2}{3}\mu^2$	1	$-\frac{2}{3}\mu^2$	$\frac{1}{2}(1 - 2\mu^2)$
M_2	For all μ and λ	$-\frac{\lambda}{\sqrt{6}}$	$\sqrt{1 + \frac{\lambda^2}{6}}$	1	$-1 - \frac{\lambda^2}{3}$	$-1 - \frac{\lambda^2}{3}$	$-\frac{1}{2}(2 + \lambda^2)$
M_3	For all μ and λ	$-\frac{\lambda}{\sqrt{6}}$	$-\sqrt{1 + \frac{\lambda^2}{6}}$	1	$-1 - \frac{\lambda^2}{3}$	$-1 - \frac{\lambda^2}{3}$	$-\frac{1}{2}(2 + \lambda^2)$
M_4	For $\mu \neq \lambda$ and $\min\{\mu^2 - \frac{3}{2}, \lambda^2 + 3\} \geq \lambda\mu$	$\frac{\sqrt{\frac{3}{2}}}{\lambda - \mu}$	$\frac{\sqrt{-\frac{3}{2} - \mu(\lambda - \mu)}}{ \lambda - \mu }$	$\frac{\mu^2 - \lambda\mu - 3}{(\lambda - \mu)^2}$	$\frac{\mu(\lambda - \mu)}{\mu^2 - \lambda\mu - 3}$	$\frac{\mu}{\lambda - \mu}$	$\frac{1}{2} \left(\frac{\lambda + 2\mu}{\lambda - \mu} \right)$

TABLE XII: The eigenvalues (λ_1, λ_2) of the Jacobian matrix corresponding to the autonomous system (89 – 90) at those critical points ($M_1 - M_4$) and the nature of the critical points.

Critical Points	λ_1	λ_2	Nature of critical Points
M_1	$-\left(\frac{3}{2} + \mu^2\right)$	$-\left(\mu^2 - \frac{3}{2}\right) + \lambda\mu$	Hyperbolic if $\left(\mu^2 - \frac{3}{2}\right) \neq \lambda\mu$, non-hyperbolic if $\left(\mu^2 - \frac{3}{2}\right) = \lambda\mu$
M_2	$-(3 + \lambda^2) + \lambda\mu$	$-\left(3 + \frac{\lambda^2}{2}\right)$	Hyperbolic if $(\lambda^2 + 3) \neq \lambda\mu$, non-hyperbolic if $(\lambda^2 + 3) = \lambda\mu$
M_3	$-(3 + \lambda^2) + \lambda\mu$	$-\left(3 + \frac{\lambda^2}{2}\right)$	Hyperbolic if $(\lambda^2 + 3) \neq \lambda\mu$, non-hyperbolic if $(\lambda^2 + 3) = \lambda\mu$
M_4	$\frac{a+d+\sqrt{(a-d)^2+4bc}}{2}$	$\frac{a+d-\sqrt{(a-d)^2+4bc}}{2}$	Hyperbolic when $\mu^2 - \frac{3}{2} > \lambda\mu$ and $\lambda^2 + 3 > \lambda\mu$, non-hyperbolic when $\mu^2 - \frac{3}{2} = \lambda\mu$ or $\lambda^2 + 3 = \lambda\mu$

Note that for the critical point M_4 we have written the eigenvalues in terms of a, b, c and d , where $a = -\frac{3}{2(\lambda-\mu)^2}(\lambda^2 + 3 - \lambda\mu)$, $b = \mp\sqrt{\frac{3}{2}}\left(\frac{3}{(\lambda-\mu)^2} + 2\right)\sqrt{-\frac{3}{2} - \mu(\lambda - \mu)}$, $c = \mp\sqrt{\frac{3}{2}}\left\{\frac{\lambda^2+3-\lambda\mu}{(\lambda-\mu)^2}\right\}\sqrt{-\frac{3}{2} - \mu(\lambda - \mu)}$, $d = -\frac{3}{(\lambda-\mu)^2}\left\{\left(\mu^2 - \frac{3}{2}\right) - \lambda\mu\right\}$.

Again, here we only state the stability of every critical points ($M_1 - M_4$) and the reason behind the stability in the tabular form, which is shown as in Table XIII.

Also note that for hyperbolic case of M_4 , the components of the Jacobian matrix a, b, c and d are very complicated and from the determination of eigenvalue, it is very difficult to provide any conclusion about the stability and for this reason we skip the stability analysis for this case.

E. Model 5: Product of exponential and power-law potential and product of exponentially-dependent and power-law-dependent dark-matter particle mass

In this consideration evolution equations in Section II can be written to the autonomous system as follows

$$x' = -3x + \frac{3}{2}x(1 - x^2 - y^2) - \sqrt{\frac{3}{2}}\lambda y^2 - \frac{\lambda}{2}y^2z - \sqrt{\frac{3}{2}}\mu(1 + x^2 - y^2) - \frac{\mu}{2}z(1 + x^2 - y^2), \quad (91)$$

$$y' = \frac{3}{2}y(1 - x^2 - y^2) - \sqrt{\frac{3}{2}}\lambda xy - \frac{\lambda}{2}xyz, \quad (92)$$

$$z' = -xz^2 \quad (93)$$

For determining the critical points corresponding to the above autonomous system, we first equate the R.H.S. of (93) with 0. Then we have either $x = 0$ or $z = 0$. For $z = 0$ then the above autonomous system converts in to the autonomous system of Model 4. So, then we will get the similar types of result as Model 4. When $x = 0$, we have three physically meaningful critical points corresponding to the above autonomous system for $\mu \neq 0$ and $\lambda \neq 0$. For another choices of μ and λ like Model 1, we will get similar types of results. The critical points are $N_1(0, 0, -\sqrt{6})$, $N_2(0, 1, -\sqrt{6})$ and $N_3(0, -1, -\sqrt{6})$ and all are hyperbolic in nature. As the x and y coordinates of these critical points are same as A_1, A_2 and A_3 and the value of cosmological parameters are not depending on z coordinate, so we get the same result for the value of cosmological parameters as A_1, A_2 and A_3 respectively, which are presented in Table I.

TABLE XIII: Table shows the stability and the reason behind the stability of the critical points ($M_1 - M_4$)

CPs	$Stability$	$Reason\ behind\ the\ stability$
M_1	<p>Stable node for $(\mu^2 - \frac{3}{2}) > \lambda\mu$</p> <p>and</p> <p>saddle node for $(\mu^2 - \frac{3}{2}) \leq \lambda\mu$</p>	<p>For $(\mu^2 - \frac{3}{2}) > \lambda\mu$, as both eigenvalues of the Jacobian matrix at M_1 are negative, so by Hartman-Grobman theorem we can conclude that the critical point M_1 is a stable node.</p> <p>For $(\mu^2 - \frac{3}{2}) < \lambda\mu$, as one eigenvalue is positive and another is negative, so by Hartman-Grobman theorem we can conclude that the critical point M_1 is a saddle node.</p> <p>For $(\mu^2 - \frac{3}{2}) = \lambda\mu$, after shifting the critical point M_1 to the origin by the coordinate transformation $(x = X - \sqrt{\frac{2}{3}}\mu, y = Y)$, the center manifold can be written as $X = \frac{1}{\mu}\sqrt{\frac{3}{2}}Y^2 + \mathcal{O}(Y^3)$ and the flow on the center manifold can be determined as $\frac{dY}{dN} = \frac{9}{4\mu^2}Y^3 + \mathcal{O}(Y^4)$. Hence, for both of the cases $\mu > 0$ and $\mu < 0$ the origin is a saddle node and unstable in nature (FIG.14).</p>
M_2, M_3	<p>Stable node for $(\lambda^2 + 3) > \lambda\mu$</p> <p>and</p> <p>saddle node for $(\lambda^2 + 3) \leq \lambda\mu$</p>	<p>For $(\lambda^2 + 3) > \lambda\mu$, as both eigenvalues of the Jacobian matrix at M_2 are negative, so by Hartman-Grobman theorem we can conclude that the critical point M_2 is a stable node.</p> <p>For $(\lambda^2 + 3) < \lambda\mu$, as one eigenvalue is positive and another is negative, so by Hartman-Grobman theorem we can conclude that the critical point M_2 is a saddle node.</p> <p>For $(\lambda^2 + 3) = \lambda\mu$, after shifting the critical point M_1 to the origin by the coordinate transformation $(x = X - \frac{\lambda}{\sqrt{6}}, y = Y \pm \sqrt{1 + \frac{\lambda^2}{6}})$, the center manifold can be written as $Y = \mp \frac{1}{2\sqrt{1 + \frac{\lambda^2}{6}}}X^2 + \mathcal{O}(X^3)$ and the flow on the center manifold can be determined as $\frac{dX}{dN} = \frac{\lambda}{2}\sqrt{\frac{3}{2}}\left\{1 - \frac{6}{\lambda^2} \pm \frac{12}{\lambda^2}\left(1 + \frac{\lambda^2}{6}\right)^{\frac{3}{2}}\right\}X^2 + \mathcal{O}(X^4)$. Hence, for all possible values λ due to the even power X in the R.H.S. of the flow equation, the origin is a saddle node and unstable in nature.</p>
M_4	<p>Saddle node for both of the cases, i.e., $\mu^2 - \frac{3}{2} = \lambda\mu$ or $\lambda^2 + 3 = \lambda\mu$</p>	<p>For $\mu^2 - \frac{3}{2} = \lambda\mu$, as M_4 converts into M_1, so we get the same stability like M_1.</p> <p>For $\lambda^2 + 3 = \lambda\mu$ as M_4 converts into M_2 and M_3, so we get the same stability like M_2 and M_3.</p>

1. Critical Point N_1

The Jacobian matrix corresponding to the autonomous system (91-93) at the critical point N_1 has three eigenvalues $\frac{3}{2}$, $-\frac{1}{4}(3 + \sqrt{9 + 48\mu})$ and $-\frac{1}{4}(3 - \sqrt{9 + 48\mu})$ and the corresponding eigenvectors are $[0, 1, 0]^T$, $[\frac{1}{24}(3 + \sqrt{9 + 48\mu}), 0, 1]^T$ and $[\frac{1}{24}(3 - \sqrt{9 + 48\mu}), 0, 1]^T$ respectively. As the critical point is hyperbolic in nature, so we use Hartman-Grobman theorem for analyzing the stability of this critical point. From the deter-

mination of eigenvalues, we conclude that the stability of the critical point N_1 depends on μ . For $\mu < -\frac{9}{48}$, the last two eigenvalues are complex conjugate with negative real parts. For $\mu \geq -\frac{9}{48}$, all eigenvalues are real.

For $\mu < -\frac{9}{48}$, due to presence of negative real parts of last two eigenvalues, yz -plane is the stable subspace and as the first eigenvalue is positive, x -axis is the unstable subspace. Hence, the critical point N_1 is saddle-focus, i.e., unstable in nature. The phase portrait in xyz coordinate system is shown as in FIG.15.

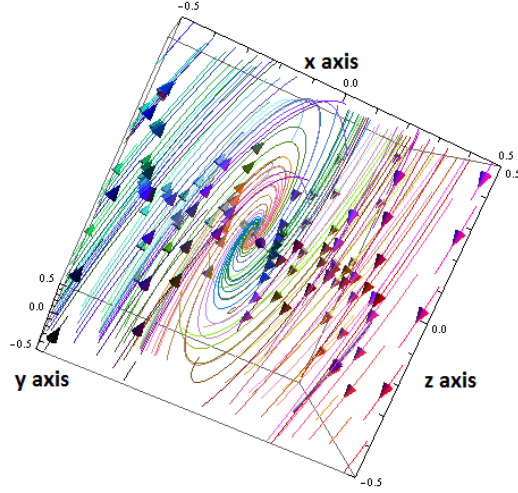


FIG. 15: Phase portrait near the origin for the critical point N_1 in xyz coordinate system. This phase portrait is drawn for $\mu = -1$.

For $\mu \geq -\frac{9}{48}$, always we have at least one positive eigenvalue and at least one negative eigenvalue and hence we can conclude that the critical point N_1 is unstable due to its saddle nature.

2. Critical Point N_2 & N_3

The Jacobian matrix corresponding to the autonomous system (91 – 93) at the critical point N_2 and N_3 has three eigenvalues -3 , $-\frac{1}{2}(3 + \sqrt{9 + 12\lambda})$ and $-\frac{1}{2}(3 - \sqrt{9 + 12\lambda})$ and the corresponding eigenvectors are $[0, 1, 0]^T$, $[\frac{1}{12}(3 + \sqrt{9 + 12\lambda}), 0, 1]^T$ and $[\frac{1}{12}(3 - \sqrt{9 + 12\lambda}), 0, 1]^T$ respectively. From the determination of the eigenvalue, we conclude that the last two eigenvalues are complex conjugate while $\lambda < -\frac{3}{4}$ and the eigenvalues are real while $\lambda \geq -\frac{3}{4}$.

For $\lambda < -\frac{3}{4}$, we can see that the last two eigenvalues are complex with negative real parts and first eigenvalue is always negative. Hence, by Hartman-Grobman theorem we conclude that the critical points N_2 and N_3 both are stable focus-node in this case. The phase portrait in xyz -coordinate system is shown as in FIG.16.

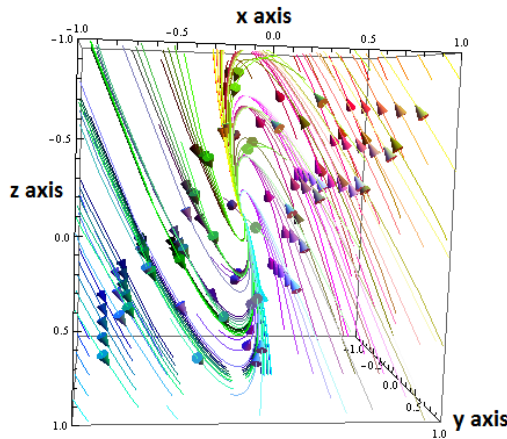


FIG. 16: Phase portrait near the origin for the critical point N_2 and N_3 in xyz coordinate system. This phase portrait is drawn for $\lambda = -1$.

For $-\frac{3}{4} \leq \lambda < 0$, we can see that all eigenvalues are negative. So, by Hartman-Grobman theorem we conclude that the critical points N_2 and N_3 both are stable node in this case.

For $\lambda > 0$, we have two negative and one positive eigenvalues. Hence, by Hartman-Grobman theorem we conclude that the critical points N_2 and N_3 both are saddle node and unstable in nature.

IV. BIFURCATION ANALYSIS BY POINCARÉ INDEX AND GLOBAL COSMOLOGICAL EVOLUTION

The flat potential plays a crucial role to obtain the bouncing solution. After the bounce, the flat potential naturally allows the universe to penetrate the slow-roll inflation regime, as a result of that making the bouncing universe compatible with observations.

In Model 1 (III A), for the inflationary scenario, we consider λ and μ very small positive number so that $V(\phi) \approx V_0$ and $M_{DM} \approx M_0$. The Eqn. (24) mainly regulate the flow along Z -axis. Due to Eqn. (24) the overall 3-dimensional phase space splits up into two compartments and the ZY -plane becomes the separatrix. In the right compartment, for $x > 0$, we have $z' < 0$ and $z' > 0$ in the left compartment. on the ZY plane $z' \approx 0$. For $\lambda \neq 0$ and $\mu \neq 0$, all critical points are located on the Y -axis. As all cosmological parameters can be expressed in terms of x and y , so we rigorously inspect the vector field on XY -plane. Due to Eqn. (15), the viable phase-space region (say S) satisfies $y^2 - x^2 \leq 1$ which is inside of a hyperbola centered at the origin (FIG.17). On the XY -plane $z' \approx 0$. So on the XY -plane, by Hartman-Grobman theorem we can conclude there are four hyperbolic sectors around A_1 (α -limit set) and one parabolic sector around each of A_2 and A_3 (ω -limit sets). So, by Bendixson theorem, it is to be noted that, the index of $A_1|_{XY}$ is 1 and the index of $A_2|_{XY}$ and $A_3|_{XY}$ is -1 . If the initial position of the universe is in left compartment and near to the α -limit, then the universe remains in the left compartment and moves towards ω -limit set asymptotically at late time. Similar phenomenon happens in right compartment also. The universe experiences a fluid dominated non-generic evolution near A_1 for $\mu > 0$ and a generic evolution for $\mu < 0$. For sufficiently flat potential, near A_2 and A_3 , a scalar field dominated non-generic and generic evolution occur for $\lambda > 0$ and $\lambda < 0$ respectively (see FIG. 18).

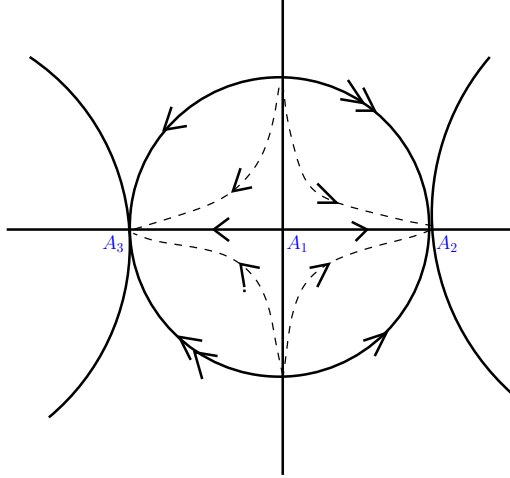


FIG. 17: Vector field on the projective plane by antipodal points identified of the disk.

The Poincaré index theorem [41] helps us to determine Euler Poincaré characteristic which is $\chi(S) = n - f - s$, where n , f , s are the number of nodes, foci and saddle on S . Henceforward we consider index as Poincaré index. So for the vector field of case-(i) $|_{XY-plane}$, $\chi(S) = 1$. This vector field can define a vector field on the projective plane, i.e., in 3-dimensional phase-space, if we consider a closed disk the XY -plane of radius one and centered at the origin, then we have the same vector field on the projective plane by antipodal point identified.

For $z = constant(\neq 0)$ plane the above characterization of vector field changes as a vertical flow along Z -axis regulate the character of the vector field. Using Bendixson theorem [41] we can find the index of nonhyperbolic critical point by restricting the vector field on a suitable two-dimensional subspace.

If we restrict ourselves on XZ -plane, A_1 is saddle in nature for $\mu > 0$. On the XZ plane the index of A_1 is -1 for $\mu > 0$ as four hyperbolic sectors are separated by two separatrices around A_1 . For $\mu < 0$, there is only one parabolic sector and the index is zero (FIG.1). On the YZ plane A_1 swap its index with XZ plane depending on the sign of μ .

On the uw -plane A_2 and A_3 have index 1 for $\lambda > 0$ and -1 for $\lambda \leq 0$. On the uw -plane A_2 and A_3 have index -1 for $\lambda > 0$ and 1 for $\lambda < 0$. At $\lambda = 0$, the index of A_2 is 0 but the index of A_3 is 1. On uv -plane the index A_2

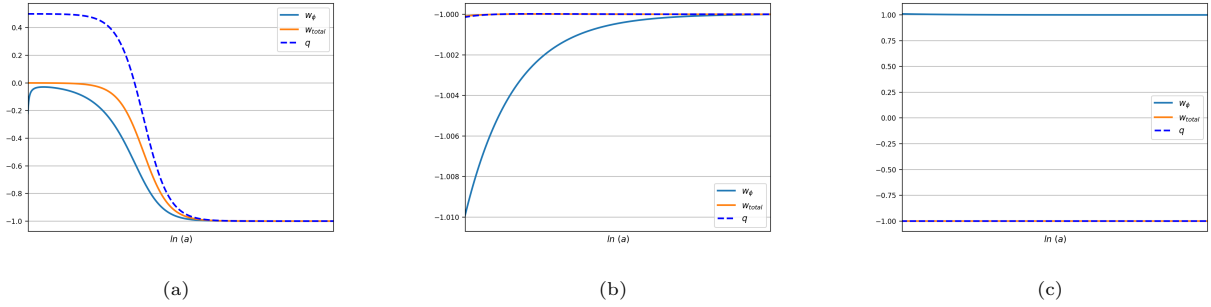


FIG. 18: *Model 1*: Qualitative evolution of the physical variables ω_{total} , ω_ϕ and q for perturbation of the parameters (λ & μ) near the bifurcation values for three sets of initial conditions. (a) The initial condition near the point A_1 . (b) The initial condition near the point A_2 . (c) The initial condition near the point A_3 . We observe that the limit of the physical parameter $\omega_{total} \rightarrow -1$. In early or present time the scalar field may be in phantom phase but the field is attracted to the de-Sitter phase.

or A_3 is 1 and does not depend on λ . On the (uw) -plane around A_2 the number of hyperbolic sector is four and there is no elliptic sector. So the index of A_2 and A_3 (*origin*) $_{|uw \text{ plane}/vw \text{ plane}}$ is -1 for $\lambda > 0$ and for $\lambda < 0$ the index is 1 as there is no hyperbolic or elliptic orbit.

A set of non-isolated equilibrium points is said to be normally hyperbolic if the only eigenvalues with zero real parts are those whose corresponding eigenvectors are tangent to the set. For the case (ii) to case (iv), we get normally hyperbolic critical points as the eigenvector $[0 \ 0 \ 1]^T$ (in new (u, v, w) coordinate system) corresponding to only zero eigenvalue, is tangent to the line of critical points. The stability of a set which is normally hyperbolic can be completely classified by considering the signs of the eigenvalues in the remaining directions. So the character of the flow of the phase space for each $z = \text{constant}$ plane is identical to the XY -plane in the previous case. Thus the system (22-24) is structurally unstable [41] at $\lambda = 0$ or $\mu = 0$ or both. On the other hand, the potential changes its character from runaway to non-runaway as λ crosses zero from positive to negative. Thus $\lambda = 0$ and $\mu = 0$ are the bifurcation values[36].

Model 2 (III B) contains five critical points $L_1 - L_5$. For $\lambda > 0$, the flow is unstable and for $\lambda < 0$ the flow on the center manifold is stable. Around L_2 , the character of the vector field same as L_1 . For $\mu = \pm\sqrt{\frac{3}{2}}$, the flow on the center manifold at L_3 or L_4 depends on the sign of λ (FIG.9 & FIG.10). On the other hand, $\mu > \sqrt{\frac{3}{2}}$ or $\mu < -\sqrt{\frac{3}{2}}$ the flow on the center manifold does not depend on λ . For $\mu > 0$, the flow on the center manifold at L_5 moves increasing direction of z . On the other hand, for $\mu < 0$, the flow on the center manifold is in decreasing direction of z . The index of L_1 is same as A_2 . For $\mu = \pm\sqrt{\frac{3}{2}}$ and $\lambda = 1$, the index of $L_2|_{XY \text{ plane}}$ is -1 as there are only four hyperbolic sectors. But for $\lambda = 2$, there are two hyperbolic and one parabolic sectors, so the index is zero. The index of L_3 is same as L_2 . The index of L_4 on ZX or XY plane is zero as there are two hyperbolic and one parabolic sector for each $\mu > 0$ and $\mu < 0$. So it is to be noted that, for $\lambda = 0, \pm\sqrt{\frac{3}{2}}$ and $\mu = 0$ the system is structurally unstable.

The universe experiences a scalar field dominated non-generic evolution near L_1 and L_2 for $\lambda > 0$ and a scalar field dominated generic evolution for $\lambda < 0$ or on the z -nullcline. Near L_3 and L_4 , a scalar field dominated non-generic evolution of the universe occur at $\mu \approx \pm\sqrt{\frac{3}{2}}$. At $\mu \approx 0$ a scaling non-generic evolution occur near L_5 (see FIG.19).

Model 3 (III C) contains three critical points $R_1 - R_3$. R_1 is saddle for all values of μ . On the xy plane the index of R_1 is same as A_1 . On the projection of the xy -plane R_2 and R_3 are stable nodes for all values of λ . On the center manifold at R_2 or R_3 , the flow is increasing direction along z -axis and the flow is decreasing direction along z -axis for $\lambda < 0$. On the XZ or YZ plane, the index of R_2 or R_3 is zero as around each of them there are two hyperbolic and one parabolic sectors. Thus we note that, for $\mu = 0$ and $\lambda = 0$, the stability of the system bifurcate.

We observe that no scaling solutions or a tracking solutions exist in this specific model like in the quintessence theory. However, the critical points which describe the de Sitter solution do not exist in the case of quintessence for the exponential potential; the universe experiences a fluid dominated non-generic evolution near critical point R_1 and a scalar field dominated non-generic evolution near critical point R_2 and R_3 . For sufficiently flat

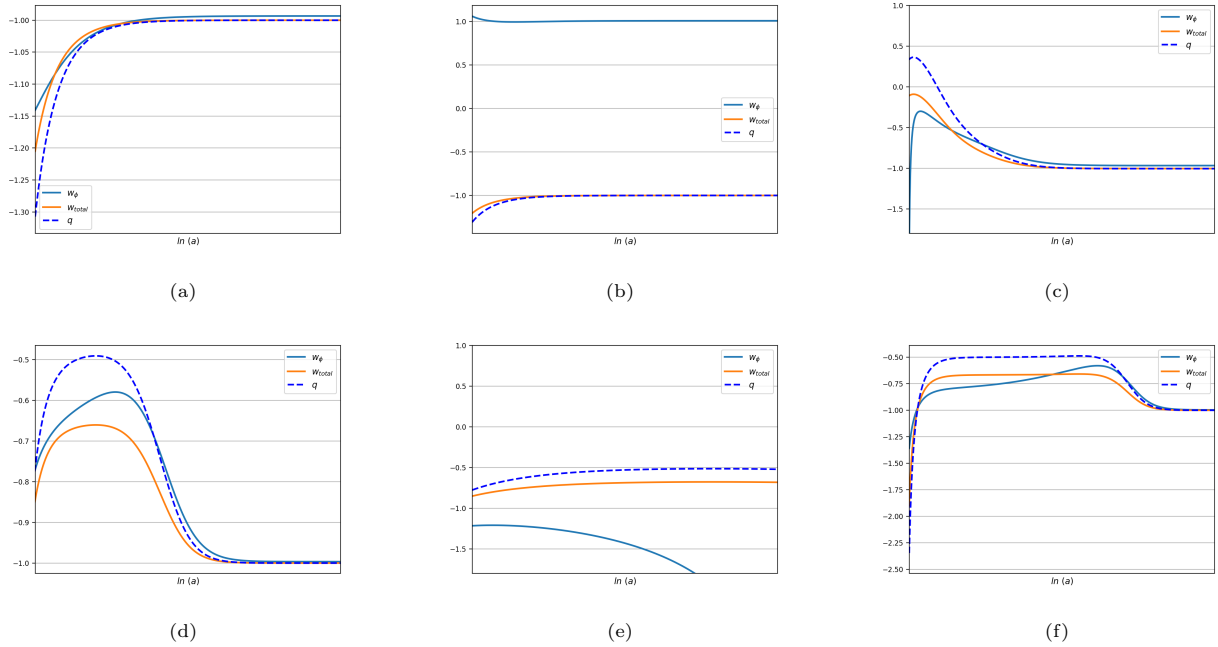


FIG. 19: *Model 2*: Some interesting qualitative evolution of the physical variables ω_{total} , ω_ϕ and q for perturbation of the parameters (λ & μ) near the bifurcation values for six sets of initial conditions. (a) The initial position near the point L_1 . (b) The initial position near the point L_2 . (c) The initial position near the point L_3 and $\mu < -\sqrt{\frac{3}{2}}$. (d) The initial position near the point L_3 and $\mu > \sqrt{\frac{3}{2}}$. (e) The initial position near the point L_4 and $\mu > \sqrt{\frac{3}{2}}$. (f) The initial position near the point L_5 and $\mu > 0$. We observe that the limit of the physical parameter $\omega_{total} \rightarrow -1$. In early or present time the scalar field may be in phantom phase but the field is attracted to the de-Sitter phase except for (b) and (e). In (e) the scalar field crosses phantom boundary line and enters into the phantom phase in late time and would cause Big-Rip.

potential, early or present phantom/non-phantom universe is attracted to Λ CDM cosmological model (see FIG. 20).

Model 4 (III D) contains four critical points $M_1 - M_4$. $M_1 - M_3$ are stable node for $(\lambda^2 + 3) > \lambda\mu$ (index 1) and saddle node (index zero) for $(\lambda^2 + 3) \leq \lambda\mu$, i.e., the stability of the system bifurcate at $(\lambda^2 + 3) = \lambda\mu$. Thus we find a generic evolution for $(\lambda^2 + 3) \neq \lambda\mu$ and no-generic otherwise. The kinetic dominated solution (M_1) and scalar field dominated solutions (M_2 and M_3) are stable for $(\lambda^2 + 3) > \lambda\mu$. For the energy density, near M_2 and M_3 , we observe that at late times the scalar field dominates $\Omega_X = \Omega_\phi \rightarrow 1$ and $\Omega_m \rightarrow 0$, while the parameter for the equation of state ω_{tot} have the limits $\omega_{tot} \rightarrow -1$ for sufficiently flat potential.

Model 5 (III E) contains three critical points N_1, N_2, N_3 . For $\mu < -\frac{3}{16}$, the Shilnikov's saddle index [42] of N_1 is $\nu_{N_1} = \frac{\rho_{N_1}}{\gamma_{N_1}} = 0.5$ and saddle value is $\sigma_{N_1} = -\rho_{N_1} + \gamma_{N_1} = 0.75$. As So Shilnikov condition [42] is satisfied as $\nu_{N_1} < 1$ and $\sigma_{N_1} > 0$. The second Shilnikov's saddle value $\sigma_{N_1}^{(2)} = -2\rho_{N_1} + \gamma_{N_1} = 0$. So, by L. Shilnikov's theorem (Shilnikov, 1965) [42] there are countably many saddle periodic orbits in a neighborhood of the homoclinic loop of the saddle-focus N_1 . As ν_{N_1} is invariant for any choice of μ , so Shilnikov's bifurcation does not appear. For $-\frac{3}{16} < \mu < 0$, the vector field near N_1 is saddle in character. On the other hand, N_1 is saddle for $\mu > 0$. So, $\mu = 0$ is a bifurcation value for the bifurcation point N_1 . Similarly, $\lambda = 0$ is a bifurcation point for the bifurcation points N_2 and N_3 . We observe scalar field dominated solutions near N_2 and N_3 which exists at bifurcation value, i.e., for sufficiently flat universe and attracted to Λ CDM cosmological model.

V. BRIEF DISCUSSION AND CONCLUDING REMARKS

The present work deals with a detailed dynamical system analysis of the interacting DM and DE cosmological model in the background of FLRW geometry. The DE is chose as a phantom scalar field with self-interacting

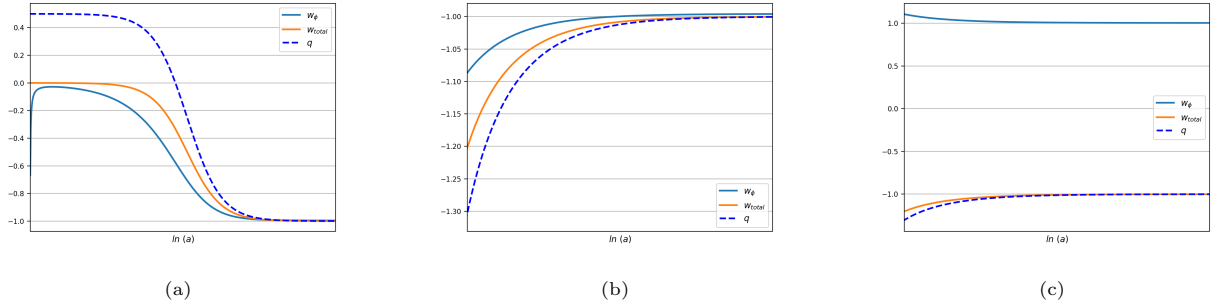


FIG. 20: Qualitative evolution of the physical variables ω_{total} , ω_ϕ and q for perturbation of the parameters (λ & μ) near the bifurcation values each of *Model 3*, *Model 4* and *Model 5* for three sets of initial conditions. The initial positions in (a), (b) and (c) are near R_1 , R_2 and R_3 (M_1 , M_2 and M_3/N_1 , N_2 and N_3) respectively.

potential while varying mass (a function of the scalar field) DM is chosen as dust. The potential of the scalar field and the varying mass of DM are chosen as exponential or power-law form (or a product of them) and five possible combination of them are studied.

Model 1: $V(\phi) = V_0\phi^{-\lambda}$, $M_{DM}(\phi) = M_0\phi^{-\mu}$

For case (i), i.e., $\mu \neq 0, \lambda \neq 0$; there are three non-hyperbolic critical points A_1, A_2, A_3 of which A_1 corresponds to DM dominated decelerating phase (dust era) while A_2 and A_3 purely DE dominated and they represent the Λ CDM model (i.e., de-Sitter phase) of the universe.

For case (ii), i.e., $\mu \neq 0, \lambda = 0$; there is one critical point and two space of critical points. The cosmological consequence of these critical points are similar to case (i).

For case (iii), i.e., $\mu = 0, \lambda \neq 0$; there is one space of critical points and two distinct critical points. But as before the cosmological analysis is identical to case (i).

For the fourth case, i.e., $\mu = 0, \lambda = 0$; there are three space of critical points (S_1, S_2, S_3) which are all non-hyperbolic in nature and are identical to the critical points in case (ii). Further, considering the vector fields in $Z = \text{constant}$ plane, it is found that for the critical point S_1 , every point on Z -axis is a saddle node while for critical points S_2 and S_3 every point on Z -axis is a stable star.

Model 2: $V(\phi) = V_0\phi^{-\lambda}$, $M_{DM}(\phi) = M_1e^{-\kappa\mu\phi}$

The autonomous system for this model has five non-hyperbolic critical points $L_i, i = 1, \dots, 5$. For L_1 and L_2 , the cosmological model is completely DE dominated and the model describes cosmic evolution at the phantom barrier. The critical points L_3 and L_4 are DE dominated cosmological solution ($\mu^2 > 3$) representing the Λ CDM model. The critical point L_5 corresponds to ghost (phantom) scalar field and it describes the cosmic evolution in phantom domain ($2\mu^2 > 3$).

Model 3: $V(\phi) = V_1e^{-\kappa\lambda\phi}$, $M_{DM}(\phi) = M_0\phi^{-\mu}$

There are three non-hyperbolic critical points in this case. The first one (i.e., R_1) is purely DM dominated cosmic evolution describing the dust era while the other two critical points (i.e., R_2, R_3) are fully dominated by DE and both describe the cosmic evolution in the phantom era.

Model 4: $V(\phi) = V_1e^{-\kappa\lambda\phi}$, $M_{DM}(\phi) = M_1e^{-\kappa\mu\phi}$

The autonomous system so formed in this case has four critical points $M_i, i = 1, \dots, 4$ which may be hyperbolic/non-hyperbolic depending on the parameters involved. The critical point M_1 represents DE as ghost scalar field and it describes the cosmic evolution in the phantom domain. For the critical points M_2 and M_3 , the cosmic evolution is fully DE dominated and is also in the phantom era. The cosmic era corresponding to the critical point M_4 describes scaling solution where both DM and DE contribute to the cosmic evolution.

Model 5: $V(\phi) = V_2\phi^{-\lambda}e^{-\kappa\lambda\phi}$, $M_{DM}(\phi) = M_2\phi^{-\mu}e^{-\kappa\mu\phi}$

This model is very similar to either model 4 or model 1, depending on the choices of the dimensionless variables x and z . For $z = 0$, the model reduces to model 4 while for $x = 0$ the model is very similar to model 1 and hence the cosmological analysis is very similar to that.

Finally, using Poincaré index theorem, Euler Poincaré characteristic is determined for bifurcation analysis of the above cases from the point of view of the cosmic evolution described by the equilibrium points. Lastly, inflationary era of cosmic evolution is studied by using bifurcation analysis.

ACKNOWLEDGMENTS

The author Soumya Chakraborty is grateful to CSIR, Govt. of India for giving Junior Research Fellowship (CSIR Award No: 09/096(1009)/2020-EMR-I) for the Ph.D work. The author S. Mishra is grateful to CSIR, Govt. of India for giving Senior Research Fellowship (CSIR Award No: 09/096 (0890)/2017-EMR-I) for the Ph.D work. The author Subenoy Chakraborty is thankful to Science and Engineering Research Board (SERB) for awarding MATRICS Research Grant support (File No: MTR/2017/000407).

-
- [1] Adam G. Riess et al. Observational evidence from supernovae for an accelerating universe and a cosmological constant. *Astron. J.*, 116:1009–1038, 1998.
 - [2] S. Perlmutter et al. Measurements of Ω and Λ from 42 high redshift supernovae. *Astrophys. J.*, 517:565–586, 1999.
 - [3] D.N. Spergel et al. First year Wilkinson Microwave Anisotropy Probe (WMAP) observations: Determination of cosmological parameters. *Astrophys. J. Suppl.*, 148:175–194, 2003.
 - [4] S.W. Allen, R.W. Schmidt, H. Ebeling, A.C. Fabian, and L. van Speybroeck. Constraints on dark energy from Chandra observations of the largest relaxed galaxy clusters. *Mon. Not. Roy. Astron. Soc.*, 353:457, 2004.
 - [5] Adam G. Riess et al. Type Ia supernova discoveries at $z > 1$ from the Hubble Space Telescope: Evidence for past deceleration and constraints on dark energy evolution. *Astrophys. J.*, 607:665–687, 2004.
 - [6] Steven Weinberg. The cosmological constant problem. *Rev. Mod. Phys.*, 61:1–23, Jan 1989.
 - [7] Robert R. Caldwell, Marc Kamionkowski, and Nevin N. Weinberg. Phantom energy and cosmic doomsday. *Phys. Rev. Lett.*, 91:071301, 2003.
 - [8] Alexander Vikman. Can dark energy evolve to the phantom? *Phys. Rev. D*, 71:023515, 2005.
 - [9] Shin'ichi Nojiri and Sergei D. Odintsov. Inhomogeneous equation of state of the universe: Phantom era, future singularity and crossing the phantom barrier. *Phys. Rev. D*, 72:023003, 2005.
 - [10] Emmanuel N. Saridakis. Phantom evolution in power-law potentials. *Nucl. Phys. B*, 819:116–126, 2009.
 - [11] M.R. Setare and E.N. Saridakis. Braneworld models with a non-minimally coupled phantom bulk field: A Simple way to obtain the -1-crossing at late times. *JCAP*, 03:002, 2009.
 - [12] Bo Feng, Xiu-Lian Wang, and Xin-Min Zhang. Dark energy constraints from the cosmic age and supernova. *Phys. Lett. B*, 607:35–41, 2005.
 - [13] Zong-Kuan Guo, Yun-Song Piao, Xin-Min Zhang, and Yuan-Zhong Zhang. Cosmological evolution of a quintom model of dark energy. *Phys. Lett. B*, 608:177–182, 2005.
 - [14] Bo Feng, Mingzhe Li, Yun-Song Piao, and Xinmin Zhang. Oscillating quintom and the recurrent universe. *Phys. Lett. B*, 634:101–105, 2006.
 - [15] Luca Amendola, Miguel Quartin, Shinji Tsujikawa, and Ioav Waga. Challenges for scaling cosmologies. *Phys. Rev. D*, 74:023525, 2006.
 - [16] Xi-ming Chen, Yun-gui Gong, and Emmanuel N. Saridakis. Phase-space analysis of interacting phantom cosmology. *JCAP*, 04:001, 2009.
 - [17] Nelson J. Nunes and D.F. Mota. Structure formation in inhomogeneous dark energy models. *Mon. Not. Roy. Astron. Soc.*, 368:751–758, 2006.
 - [18] T. Clifton and John D. Barrow. The Ups and downs of cyclic universes. *Phys. Rev. D*, 75:043515, 2007.
 - [19] Chen Xu, Emmanuel N. Saridakis, and Genly Leon. Phase-Space analysis of Teleparallel Dark Energy. *JCAP*, 07:005, 2012.
 - [20] Hong-Sheng Zhang and Zong-Hong Zhu. Interacting chaplygin gas. *Phys. Rev. D*, 73:043518, 2006.
 - [21] Carlos R. Fadrags and Genly Leon. Some remarks about non-minimally coupled scalar field models. *Class. Quant. Grav.*, 31(19):195011, 2014.
 - [22] Tame Gonzalez and Israel Quiros. Exact models with non-minimal interaction between dark matter and (either phantom or quintessence) dark energy. *Class. Quant. Grav.*, 25:175019, 2008.
 - [23] Greg W. Anderson and Sean M. Carroll. Dark matter with time dependent mass. In *1st International Conference on Particle Physics and the Early Universe*, pages 227–229, 9 1997.
 - [24] T. Damour, G. W. Gibbons, and C. Gundlach. Dark matter, time-varying g , and a dilaton field. *Phys. Rev. Lett.*, 64:123–126, Jan 1990.
 - [25] Glennys R. Farrar and P. James E. Peebles. Interacting dark matter and dark energy. *Astrophys. J.*, 604:1–11, 2004.
 - [26] Mark B. Hoffman. Cosmological constraints on a dark matter – dark energy interaction. *arXiv: Astrophysics*, 7 2003.
 - [27] Xin Zhang. Coupled quintessence in a power-law case and the cosmic coincidence problem. *Mod. Phys. Lett. A*, 20:2575, 2005.
 - [28] Micheal S. Berger and Hamed Shojaei. Interacting dark energy and the cosmic coincidence problem. *Phys. Rev. D*, 73:083528, 2006.
 - [29] Luca Amendola and Domenico Tocchini-Valentini. Baryon bias and structure formation in an accelerating universe. *Phys. Rev. D*, 66:043528, Aug 2002.

- [30] Massimo Pietroni. Brane worlds and the cosmic coincidence problem. *Phys. Rev. D*, 67:103523, May 2003.
- [31] Luca Amendola, Gabriela Camargo Campos, and Rogerio Rosenfeld. Consequences of dark matter-dark energy interaction on cosmological parameters derived from type ia supernova data. *Phys. Rev. D*, 75:083506, Apr 2007.
- [32] Luca Amendola. Coupled quintessence. *Phys. Rev. D*, 62:043511, 2000.
- [33] D. Comelli, M. Pietroni, and A. Riotto. Dark energy and dark matter. *Phys. Lett. B*, 571:115–120, 2003.
- [34] Urbano França and Rogerio Rosenfeld. Age constraints and fine tuning in variable-mass particle models. *Phys. Rev. D*, 69:063517, Mar 2004.
- [35] Sudip Mishra and Subenoy Chakraborty. Stability and bifurcation analysis of interacting $f(T)$ cosmology. *Eur. Phys. J.*, C79(4):328, 2019.
- [36] Sudip Mishra and Subenoy Chakraborty. A non-canonical scalar field cosmological model: Stability and bifurcation analysis. *Mod. Phys. Lett.*, A34(32):1950261, 2019.
- [37] Sudip Mishra and Subenoy Chakraborty. Dynamical system analysis of Einstein–Skyrme model in a Kantowski–Sachs spacetime. *Annals Phys.*, 406:207–219, 2019.
- [38] Genly Leon and Emmanuel N. Saridakis. Phantom dark energy with varying-mass dark matter particles: acceleration and cosmic coincidence problem. *Phys. Lett. B*, 693:1–10, 2010.
- [39] Soumya Chakraborty, Sudip Mishra, and Subenoy Chakraborty. Dynamical system analysis of three-form field dark energy model with baryonic matter. *Eur. Phys. J.*, C80(9):852, 2020.
- [40] Christian G. Boehmer, Nyein Chan, and Ruth Lazkoz. Dynamics of dark energy models and centre manifolds. *Phys. Lett. B*, 714:11–17, 2012.
- [41] Lawrence Perko. *Differential equations and Dynamical systems*. Springer-Verlag, New York. Inc., Third edition, 1991.
- [42] LP Shilnikov and Andrey Shilnikov. Shilnikov bifurcation. *Schopedia*, 2007. <https://www.researchgate.net/publication/220580167>.